

Effect of Edge Beam Deformations on the Slab Panel Method

By

Taidi Gu

Supervised by:

Dr Anthony K. Abu

Associate Professor G Charles Clifton

A thesis submitted in partial fulfilment of the requirements for the degree of
Master of Engineering in Fire Engineering

Department of Civil and Natural Resources Engineering
University of Canterbury
Private Bag 4800
Christchurch, New Zealand

MAY 2016

ABSTRACT

Previous accidental fires in multi-storey buildings and large scale fire tests have shown composite floors with unprotected steel beams had large deformations but collapse did not occur due to a mechanism known as tensile membrane action. The Slab Panel Method (SPM) was developed as a simplified performance-based design method including tensile membrane action for everyday design.

As SPM has some provisions of edge beam deformations in its analysis, this research was carried out to assess how realistic these provisions are. The study was performed on SPM and VULCAN, which is a non-linear finite element program that includes both thermal and structural analysis. The effect of various edge continuity conditions on the basic slab panel was assessed by VULCAN models and compared with SPM. 9 m x 9 m slab panel were firstly investigated, then 9 m x 6 m and 9 m x 12 m slab panels were modelled to investigate the effect of aspect ratio on SPM's provisions.

The VULCAN analyses showed that the slab panels perform better with more internal edges and edge beam deformations are always critical to the fire resistance of the slab panels. The SPM and VULCAN deflections were in good agreement in the 9 m x 9 m slab panel, but it underestimates the deflections of 9 m x 6 m slab panel and was slightly conservative on the 9 m x 12 m slab panel.

It is concluded that slab continuity over the edge beams significantly enhanced the fire resistance of the slab panel. SPM provided good estimates on the fire resistance of slab panel when the edge beams are designed to be very strong or well protected, but underestimated the external edge beam deformations. It is recommended that when using the SPM in design, the external edge beams need to be designed for higher loadings than just from the yield line tributary area and that for irregular panels or high variable loading Finite Element Analysis (FEA) software is recommended to check the results.

Deputy Vice-Chancellor's Office
Postgraduate Office

Co-Authorship Form

This form is to accompany the submission of any thesis that contains research reported in co-authored work that has been published, accepted for publication, or submitted for publication. A copy of this form should be included for each co-authored work that is included in the thesis. Completed forms should be included at the front (after the thesis abstract) of each copy of the thesis submitted for examination and library deposit.

Please indicate the chapter/section/pages of this thesis that are extracted from co-authored work and provide details of the publication or submission from the extract comes:

Figures from Page 58, 65, 74, 75 was extracted from the co-authored work: Gu, T., Abu, A.K. and Clifton, G.C. (2013) Effect of Edge Beam Deformations on the Fire Resistance of Steel-Concrete Composite Floors. Singapore: 10th Pacific Structural Steel Conference (PSSC 2013), 8-11 Oct 2013. : 528-533. <http://dx.doi.org/10.3850/978-981-07-7137-9> 221.

Please detail the nature and extent (%) of contribution by the candidate:

My contribution was being involved with fire modelling and writing the paper. The extent of the contribution was 75%.

Certification by Co-authors:

If there is more than one co-author then a single co-author can sign on behalf of all

The undersigned certifies that:

- The above statement correctly reflects the nature and extent of the Candidate's contribution to this co-authored work
- In cases where the candidate was the lead author of the co-authored work he or she wrote the text

Name: Taidi Gu

Signature: 

Date: 29/04/16

Name: *Antony Abu*

Signature: 

Date: 29/04/16

(on behalf of all other co-authors)

ACKNOWLEDGEMENTS

I would like to thank all the people who inspired and assisted me in any possible way that made it possible to complete this thesis.

I would like to sincerely thank my supervisors, Dr Anthony Abu and Associate Professor Charles Clifton, for their guidance, support and encouragement throughout the course of this thesis.

I would like to extend my deep appreciation to Associate Professor Michael Spearpoint and Professor Charles Fleischmann for invaluable help and guidance throughout the Fire Engineering Programme.

I would like to thank all my friends in the Fire Engineering programme for sharing their knowledge and help with my thesis and general study.

I would like to thank Dr James O'Neil for his invaluable ideas and help with use of the finite element software, ABAQUS.

I am grateful to the financial support and sponsorship from the New Zealand Fire Service.

Finally, my greatest tanks go to my wife Mona Liu for her love, patience, support and encouragement throughout the write-up of this thesis.

TABLE OF CONTENTS

Abstract.....	i
Acknowledgements.....	iii
List of Figures	vi
List of Tables	ix
1 Introduction	1
1.1 Background.....	1
1.2 Objectives.....	3
1.3 Outline.....	4
2 Design of Composite Floors in Fire	5
Introduction	5
2.1 Traditional Design in Fire Conditions	5
2.1.1 Design at ambient temperature	5
2.1.2 Design of composite floors for severe fire.....	7
2.1.3 Advanced calculation methods.....	11
2.2 Observation of the behaviour of composite floors in fire	12
2.2.1 Broadgate fire	12
2.2.1 Cardington full-scale fire tests	14
2.3 Tensile Membrane Action	16
2.3.1 History of Tensile Membrane Action	17
2.3.2 BRE Garston ambient temperature concrete slab test.....	18
2.4 Design methods with Tensile Membrane Action	19
2.4.1 Bailey – BRE method	20
2.4.2 The Slab Panel Method (SPM)	22
2.5 The VULCAN FINITE ELEMENT PACKAGE	25
2.6 Limitation of the Simple Methods	30

2.7	Impetus of the current research	32
3	Methodology.....	33
	Introduction	33
3.1	Floor Description	33
3.2	The Slab Panel Method (SPM) Setup	37
3.2.1	The SPM Thermal Analysis.....	37
3.2.2	SPM structural analysis	41
3.3	VULCAN Analysis	45
3.3.1	VULCAN Thermal Analysis.....	45
3.3.2	VULCAN Structural Analysis	51
3.4	Comparisons.....	66
3.4.1	Edge Beam Stability under Various Slab Continuities.....	66
3.4.2	Aspect Ratio	68
	Conclusion.....	69
4	Comparisons of VULCAN and the SPM models	71
	Introduction	71
4.1	Edge Beam Stability under Various Continuities.....	71
4.2	Re-Designed Edge Beam Stability under Various Continuities	79
4.3	Comparisons of SPM Required Deflection and VULCAN	83
4.4	Effect of Aspect Ratio	86
	Introduction	86
4.4.1	Slab Panels Description.....	86
4.4.2	9m x 12m Slab Panel	87
4.4.3	9 m x 6 m Slab Panel	90
	Conclusions	92
5	Conclusions and Recommendations.....	93
5.1	Recommendations for future research.....	95
	References	97

LIST OF FIGURES

FIGURE 2-1: COMPOSITE STEEL-CONCRETE FLOOR SYSTEM (CLIFTON, 2006)	6
FIGURE 2-2: STANDARD FIRE TEMPERATURE-TIME CURVE.....	9
FIGURE 2-3: BUCKLED COLUMN FROM THE BROADGATE FIRE (LAWSON <i>ET AL.</i> , 1991).....	13
FIGURE 2-4: FLOORS EXPERIENCED LARGE VERTICAL DEFLECTIONS (NEWMAN <i>ET AL.</i> , 2000)	15
FIGURE 2-5: TENSILE MEMBRANE ACTION OF A SIMPLY SUPPORTED SLAB (BAILEY AND TOH, 2007)	16
FIGURE 2-6 : YIELD LINE CRACK PATTERN IN AMBIENT TEMPERATURE LOADING TEST (SAWCZUK & WINNICKI, 1965).	17
FIGURE 2-7: FULL DEPTH CRACK FORMING IN THE CENTRAL SLAB (BAILEY, 2000).	19
FIGURE 2-8: DIVISION OF FLOOR INTO SLAB PANELS WITH UNPROTECTED BEAMS (BAILEY, 2003)	21
FIGURE 2-9: FLOOR PLAN SHOWING DIMENSIONS FOR YIELD LINE PATTERN AND DEVELOPED MOMENTS (CLIFTON, 2006)	23
FIGURE 2-10: THREE STAGES OF DEFLECTION IN FIRE.....	25
FIGURE 2-11: VULCAN CAN MODEL THE STRUCTURAL FIRE BEHAVIOR IN 3D, FROM VULCAN-SOLUTION.COM	26
FIGURE 2-12: SLAB AND BEAM ELEMENTS IN VULCAN (HUANG, 2010).....	27
FIGURE 2-13: TRAPEZOIDAL COMPOSITE SLAB PROFILE	28
FIGURE 2-14: VULCAN THERMAL ANALYSIS METHODS.....	28
FIGURE 2-15: SLAB PANEL FOLDING MECHANISM (ABU <i>ET AL.</i> , 2012)	31
FIGURE 3-1: CONCRETE TRAPEZOIDAL SLAB PROFILE (ABU <i>ET AL.</i> , 2012)	34
FIGURE 3-2: 9 M × 9 M ISOLATED SLAB PANEL WITH PROTECTED AND UNPROTECTED STEEL BEAMS (GU <i>ET AL.</i> , 2013)	34
FIGURE 3-3: MESH POSITION AND HEAT FLOW PATH FOR MESH TEMPERATURE DISTRIBUTION (CLIFTON, 2006)...	38
FIGURE 3-4: SPM PREDICTED TEMPERATURE AGAINST TIME	39

FIGURE 3-5: DEVELOPMENT OF POSITIVE MOMENT CAPACITY IN X-DIRECTION BY UNPROTECTED SECONDARY BEAMS AND REINFORCEMENT (CLIFTON, 2006).....	43
FIGURE 3-6: FLOOR PLAN SHOWING EXTERNAL AND INTERNAL EDGES (CLIFTON, 2006)	44
FIGURE 3-7: UNPROTECTED AND PROTECTED STEEL BEAMS UNDER STANDARD FIRE EXPOSURE.....	46
FIGURE 3-8: COMPARISONS BETWEEN THE FPRCBC-T RESULTS AND SPM.....	48
FIGURE 3-9: COMPARISONS BETWEEN THE RESULTS FROM ABAQUS THERMAL AND SPM	49
FIGURE 3-10: (A) CROSS-SECTION WITH LAYERS (LEFT) AND (B) TEMPERATURE CURVES OF THE LAYERS (RIGHT) ...	50
FIGURE 3-11: COMPARISON BETWEEN VULCAN MODEL AND GASTON TEST DATA	54
FIGURE 3-12: 9 M × 9 M MODELLED IN VULCAN.....	56
FIGURE 3-13: SPM LIMITING DEFLECTION AND MAXIMUM DEFLECTION.....	57
FIGURE 3-14: CENTRAL AND EDGE BEAM DEFLECTIONS OF 9 M × 9 M ISOLATED SLAB PANEL	59
FIGURE 3-15: ISOLATED SLAB PANEL MIDSPAN AND EDGE BEAM RELATIVE DEFLECTIONS (GU <i>ET AL</i> , 2013)	60
FIGURE 3-16: COMPARISON BETWEEN MIDSPAN DEFLECTIONS OF SLAB PANEL (V2) WITH CORNER VERTICAL RESTRAINT AND CONSTANT VERTICAL SUPPORT AROUND THE EDGES	62
FIGURE 3-17: COMPARISON BETWEEN DEFLECTIONS OF ISOLATED SLAB PANEL AND SLAB PANEL (V3) WITH OVERPROTECTED EDGES.....	63
FIGURE 3-18: COMPARISON BETWEEN DEFLECTIONS OF ISOLATED SLAB PANEL AND SLAB PANE WITH COLD EDGES	64
FIGURE 3-19: COMPARISONS BETWEEN PRIMARY BEAM DEFLECTIONS	65
FIGURE 3-20: COMPARISONS BETWEEN SECONDARY BEAM DEFLECTIONS	65
FIGURE 3-21: 9 M × 9 M SLAB PANELS WITH DIFFERENT NUMBER OF CONTINUITY FROM S1 TO S6 (GU <i>ET AL</i> , 2013)	67
FIGURE 3-22: THREE SIZES SLAB PANELS ARE MODELLED IN THIS RESEARCH (ABU <i>ET AL.</i> , 2012)	68
FIGURE 4-1: S2 CENTRAL AND NON-CONTINUOUS PRIMARY AND SECONDARY BEAM DEFLECTION.....	72
FIGURE 4-2: S2 CONTINUOUS SECONDARY AND PRIMARY BEAMS DEFLECTION	73
FIGURE 4-3: S3 CENTRAL AND NON-CONTINUOUS PRIMARY BEAM DEFLECTION.....	74

FIGURE 4-4: S5 CENTRAL AND NON-CONTINUOUS PRIMARY BEAM DEFLECTIONS.....	74
FIGURE 4-5: COMPARISON BETWEEN S3 AND S5 DEFLECTIONS	75
FIGURE 4-6: S4 CENTRAL DEFLECTION.....	76
FIGURE 4-7: S6 CENTRAL AND NON-CONTINUOUS PRIMARY BEAM DEFLECTION.....	76
FIGURE 4-8: CENTRAL VERTICAL DEFLECTION OF A SLAB PANEL WITH TWO CONTINUOUS SIDES (GU ET AL, 2013)	77
FIGURE 4-9: CENTRAL VERTICAL DEFLECTIONS OF THE SLAB PANEL WITH VARIOUS CONTINUITIES (GU ET AL, 2013)	78
FIGURE 4-10: SPM YIELD-LINE PATTERN USED IN EDGE BEAM DESIGN (CLIFTON, 2002)	80
FIGURE 4-11: REDESIGNED 9 M × 9 M SLAB PANEL.....	80
FIGURE 4-12: COMPARISON OF ORIGINAL SLAB PANEL AND RE-DESIGNED SLAB PANEL.....	81
FIGURE 4-13: CENTRAL VERTICAL DEFLECTION OF A SLAB PANEL WITH TWO CONTINUOUS SIDES. (LEFT: ORIGINAL DESIGN SLAB PANEL. RIGHT: RE-DESIGNED SLAB PANEL).....	82
FIGURE 4-14: CENTRAL VERTICAL DEFLECTION OF A SLAB PANEL WITH VARIOUS CONTINUITIES. (LEFT: ORIGINAL DESIGNED SLAB PANEL. RIGHT: RE-DESIGNED SLAB PANEL)	82
FIGURE 4-15: SPM – 9 M × 9 M SLAB PANEL, REQUIRED DEFLECTIONS (LEFT) AND VULCAN – 9 M × 9 M SLAB PANEL, CENTRAL VERTICAL DEFLECTIONS (RIGHT).	85
FIGURE 4-16: 9 M × 12 M COMPARISON BETWEEN VULCAN AND SPM CENTRAL DEFLECTION	88
FIGURE 4-17: 9 M × 12 M SLAB PANELS WITH DIFFERENT NUMBER OF INTERNAL EDGES FROM S1 TO S6.....	88
FIGURE 4-18: SPM – 9 M × 12 M SLAB PANEL, REQUIRED DEFLECTIONS (LEFT) AND VULCAN – 9 M × 9 M SLAB PANEL, CENTRAL VERTICAL DEFLECTIONS (RIGHT).	89
FIGURE 4-19: 9 M × 6 M COMPARISON BETWEEN THE SPM AND THE VULCAN CENTRAL DEFLECTION	90
FIGURE 4-20: 9 M × 6 M SLAB PANELS WITH DIFFERENT NUMBER OF INTERNAL EDGES FROM S1 TO S6.....	91
FIGURE 4-21: SPM – 9 M × 6 M SLAB PANEL, REQUIRED DEFLECTION(LEFT) AND VULCAN – 9 M × 6 M SLAB PANEL, CENTRAL VERTICAL DEFLECTION (RIGHT).	91

LIST OF TABLES

TABLE 3-1: DESIGN LOADING.....	35
TABLE 3-2: DESIGN TEMPERATURES OF UNPROTECTED SECONDARY BEAM ELEMENTS (CLIFTON, 2006).....	41
TABLE 3-3: RELATIONSHIP BETWEEN $f_{ysb\theta}$ AND f_{ysb20} FOR UNPROTECTED SECONDARY BEAMS (CLIFTON, 2006)	42
TABLE 3-4: CALCULATED THICKNESS FROM ES, ED AND TCT	47
TABLE 3-5: VULCAN ANALYSIS AND PARAMETERS	56
TABLE 4-1: EDGE BEAM DESIGN DATA FOR 60 MINUTES FIRE RESISTANCE RATING	87

1 INTRODUCTION

1.1 Background

Steel-concrete composite floors are structural members that are made up of reinforced concrete slabs acting compositely with steel-decking and supported on a gridwork of steel beams. The primary advantage of this system is that it can be installed over large areas without using reusable formwork and heavy lifting equipment so costs can be saved. In addition, the light construction results in lighter foundations. For these reasons steel-concrete composite floors are popular in multi-storey steel framed construction.

When fires occur the structural system should still carry its applied loading even with reduction of strength. Steel is a good conductor of heat, and so loses its strength rapidly on exposure to fire. As such composite floors may require applied protection for fire resistance, to ensure they prevent fire and smoke spread and carry their applied loads as well.

To protect composite floors from fire, the traditional method has been to prescribe applied fire protection on all exposed steelwork, based on individual member capacities. However, this method does not consider interactions between parts of the steel structure. From accidental fires in multi-storey buildings and large scale fire tests, composite floors with unprotected steel beams showed large deformations but no collapse after severe fires, due to a mechanism known as tensile membrane action. It has been found that this behaviour can be incorporated into a performance-based design of steel-framed structures where a large number of floor beams can be left unprotected. It is more economical to use tensile membrane action in

structural fire design compared with the traditional design methods. Previous research has shown that Finite Element Analysis (FEA) software, such as VULCAN (Huang et al., 2003a; 2003b), SAFIR (Franssen, 2003) and ABAQUS are capable of modelling tensile membrane action. However, FEA simulation requires complex user knowledge and time to obtain results. Therefore, simplified methods that can provide good predictions of structural behaviour, but include consideration of tensile membrane behaviour of these slabs and are suitable for everyday design, have been developed. The Slab Panel Method (SPM) is one such simplified fire design tool for steel-concrete composite floors. It has been developed since 2001, by Clifton (2001) in New Zealand, with the current version (Clifton, 2006) now in use. It has been applied to many steel framed buildings in the New Zealand over the last 8 years and has been used to a limited extent in Australia and the UK.

The SPM divides the composite floor into several rectangular slab panels which are designed as whole units, and each slab panel consists of protected edge beams and unprotected interior beams. It is implemented by a simple spreadsheet model that calculates the enhancement of tensile membrane action in addition to the traditional yield-line capacity of the slab. Inherent in the simple method is the assumption that protected edge beams maintain their vertical support throughout fire exposure.

In reality, the edge beams always deflect and slabs usually extend beyond a single slab panel. Axial restraints from the continuous edges enhance the vertical supports along those edges. Previous research (Abu *et al.*, 2008) has indicated that the assumption of the simple methods is not sufficiently conservative, because the deflection of the edge beams would reduce the total fire resistance of the slab. Through a series of investigations of isolated slab panels with various

edge support conditions, Abu *et al* (2008, 2010, and 2011) found that the edge beam stiffness must function as effective stiff supports in order to generate the two-way tensile membrane action. More importantly, the deflection of edge beams may cause a premature edge beam failure of the slab panel if the deflection is too large.

The SPM has some provision of edge beam deformation in its analysis. However, research on SPM has not investigated its suitability for modelling continuous edges. As such this research seeks to quantify the effectiveness of edge-beam support in the SPM where continuity is concerned.

1.2 Objectives

The objectives of this research are:

1. To examine the effect of edge beam deformations under various continuity conditions on the basic slab panel design using finite element models.
2. To assess the suitability of the current SPM in predicting slab panel fire resistance under various support conditions in fire.
3. To investigate the effects of aspect ratio on edge-beam stability of the slab panel method.

1.3 Outline

This research consists of five chapters. The description of each chapter is outlined within this section.

- Chapter 1 has already given a brief introduction and outlines the objectives of this research.
- Chapter 2 summaries the behaviour the steel – concrete composite floor including previous research and findings of tensile membrane action.
- Chapter 3 introduces VULCAN and the SPM which are later compared in the thesis. It also describes the procedure of developing a 9m x 9m slab panel using VULCAN and the SPM. It details the input for developing the 9m x 9m slab panel within VULCAN and the SPM. This 9 m x 9 m slab panel will be used for comparisons in the later chapters.
- Chapter 4 presents the results of the 9m x 9m slab panel from VULCAN and SPM. It compares the SPM predictions with VULCAN results and discusses the influences on the edge beam stability from different support conditions. It also investigates the effects of aspect ratio on edge-beam stability by examining VULCAN modelling results from three slab panel sizes (9 m x 6 m, 9m x 9m and 9 m x 12 m) and comparing them with the SPM results.
- Chapter 5 provides a conclusion of this research and makes recommendation for future work.

2 DESIGN OF COMPOSITE FLOORS IN FIRE

Introduction

This chapter presents background literature of this research. It covers traditional design methods of composite floors in fire, the observations of the behaviour of composite floors and the use of the tensile membrane action for design of composite slabs in fire. It also explains the motivation behind this research and introduces the computer programs SPM and VULCAN, which are used in this research.

2.1 Traditional Design in Fire Conditions

2.1.1 Design at ambient temperature

Current structural design codes adopt limit state design philosophy. A limit state is a condition beyond which a structure no longer meets the relevant design criteria. There are generally two classes of limit states: Ultimate Limit State (ULS) and Serviceability Limit State (SLS). The ULS considers the ultimate load carrying capacity of the structure. If the applied design action exceeds the load carrying capacity, a structural collapse will occur. The SLS considers excessive deflection or vibration in structural members. If deflection or vibration criteria are exceeded in the in-service condition, a structure will not collapse, but will suffer loss of amenity, therefore violating the requirement of the New Zealand Building Code Clause B1.

Within composite steel-concrete floors, concrete slabs sit on secondary beams, which are supported by the primary beams, which are in turn supported between steel columns as shown in Figure 2-1.

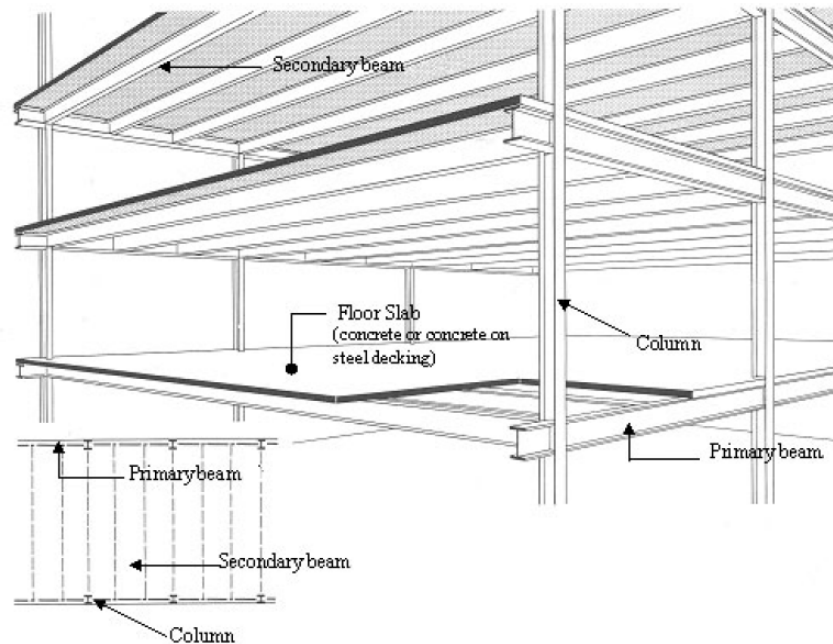


Figure 2-1: Composite steel-concrete floor system (Clifton, 2006)

Steel and concrete are two major structural materials used in construction. Each of the materials has its own characteristics, strengths and weaknesses. Steel elements are usually made of thin plates due to its high strength to weight ratio, and these are prone to local bulking under compression. On the other hand, concrete elements are thick and hard to buckle, but they have weak tensile strength, therefore reinforcing bars are placed within concrete to overcome the problem. Reinforced concrete slabs have good sound and fire insulation properties, and they are usually supported by steel beams. To sufficiently use the properties of these two materials, steel sections are connected to reinforced concrete sections so that the two structural members act as one. A composite beam consists of a steel beam and a concrete slab with shear connectors between them. For positive bending, concrete slabs make up the compression flange and effectively restrain the horizontal movement of the steel beam flange.

Therefore only the maximum bending moment capacity governs (Wang, 2002). Composite beams can be designed to act nominally simply supported in one way bending between the supporting secondary steel beam. The tension force induced by bending is carried by the steel decking acting compositely with the concrete slab. Reinforcement is added within the concrete slab to control cracking. Design methods for composite steel beams can be found in national design codes. Eurocode 4 (CEN, 2005) and NZS3404 (SNZ, 2006) specify the requirements and methods of designing composite beams in Europe and New Zealand, respectively. Typically, the design for fire follows on from the room-temperature design.

2.1.2 Design of composite floors for severe fire

2.1.2.1 Failure criteria in fire

When fire occurs, building elements need to have a level of fire resistance to prevent failure. Three failure criteria - stability, integrity and insulation are used to address the fire resistance rating of construction elements. To meet the stability criterion, primary elements such as columns, beams, floors and load bearing walls must carry their applied loads within the required fire resistance time. To meet the integrity criterion, structural elements must prevent the penetration of fire and smoke during the fire. And to meet the insulation criterion, the unexposed side must not exceed an average temperature rise of 140°C and a local maximum rise of 180°C within the specified fire resistance period. For composite floors, all three criteria must be satisfied in the design process, because they are load-bearing separating elements.

2.1.2.2 Fire Resistance Rating (FRR)

In order to assess those three criteria, the building elements exposed to fire shall allow adequate time for people to evacuate safely and allow fire service personnel to undertake rescue and firefighting operations. The design time that assigned to a building element is the Fire Resistance Rating (FRR). The FRR in the buildings depends on the fire engineering design of the building. According to current New Zealand Building Code (NZBC) compliance document Acceptable Solution C/AS 1-7, the FRR is determined by whether the building is sprinkler protected. For example, an office building with sprinklers requires 30min FRR for internal fire separation but it will require 60min FRR without sprinkler protection.

The FRR within a building element is determined by the time exposed in a fire test (England *et al*, 2000). The standard fire, or ISO834 fire (ISO, 1999) is the international standard of experimental fire tests, the temperature T (°C) at day time in the furnace given by:

$$T = 345\log_{10}(8t + 1) + T_0$$

Where t is the time (min) and T_0 is the ambient temperature (°C). The typical standard fire temperature curve is shown in Figure 2-2 below, with $T_0 = 20^\circ\text{C}$.

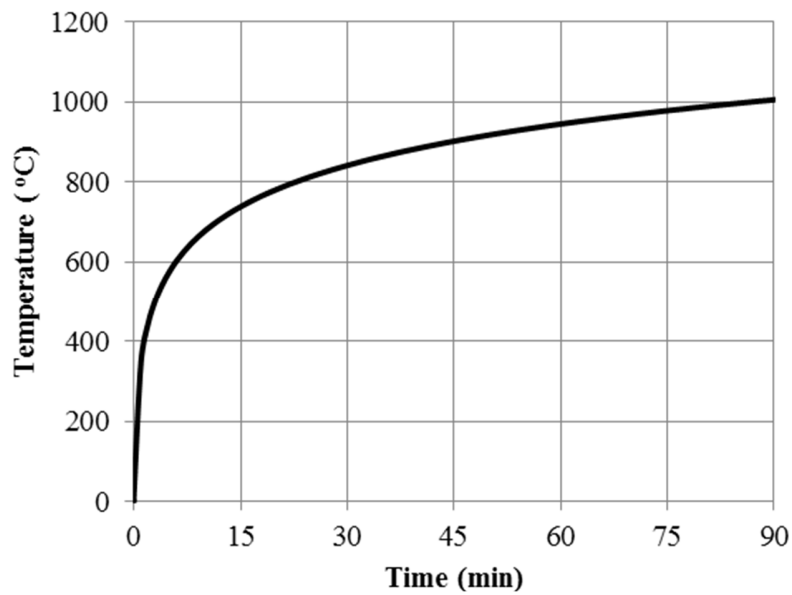


Figure 2-2: Standard fire temperature-time curve.

Similar to the ambient temperature design, it is important to assess the load-carrying capacity of structural members in fire. Several methods have been developed to assess the fire resistance of composite floors.

2.1.2.3 Tabulated data

The tabulated data are a set of design criteria that are not derived from any calculations that ensure minimum fire resistance of elements. Many national design codes provide tabulated data for fire protection of structural members. They directly give the material and thickness of protection for a specific fire resistance time.

Tabulated data for steel-concrete composite floors are presented in design standards. For example, NZS3101 (SNZ, 2006) gives tabulated data of minimum thickness of concrete and their corresponding fire resistance rating; e.g. designing flat slabs with 60 minutes FRR shall have 180mm slab thickness and 15mm axis distance.

Tabulated data are easy and fast to use, but they may be less conservative because they do not make allowance for the level of load (Buchanan, 2001), and are only based on the standard fire test (Franssen *et al*, 2009). To provide quantifiable fire resistance rating but also easy to use, simplified calculation methods can be used in everyday design. Also tabulated data for reinforced concrete members are based on flexural mode of failure which may not always be the governing failure mode.

2.1.2.4 Simplified calculation methods

Simplified calculation methods are the methods that are simple enough to apply to routine design without using a sophisticated computer program (Frassen *et al*, 2009). They are developed based on similar procedure of conventional structural design which is easy for structural engineers to use. They can be classified into time domain, strength domain and temperature domain. They all require calculated design resistance, R_{fire}^* to be greater than the design action U_{fire}^* under fire condition, within the required fire design time.

The time domain calculates the failure time that can obtained from a time equivalent formula when the fire load and ventilation parameters are known (Buchanan, 2001). This is then compared with the required fire resistance time. The strength domain considers the structure behaviour in fire situation similar to room temperature design. Eurocode 3 (CEN, 2005) provides reduction factors for yield strength of steel at elevated temperature. Eurocode 2 and 4 provide reinforcement data. Especially for composite slabs and beams, a bending moment resistance method is provided by Eurocode 4 (CEN, 2005).

The temperature domain calculates the limiting temperature which is the temperature at which the load-carrying capacity of the member would be lost. It compares the limiting temperature with the maximum temperature reached within the required duration of exposure. New Zealand Steel Standard uses this method and the time when the steel beam reach the limiting steel temperature in standard fire is called Period OF Structural Adequacy (PSA) in the New Zealand Steel Standard NZS3404 (SNZ, 1997). Eurocode 3 (CEN, 2005) also provides equations to calculate the critical temperature.

The simplified methods are easy to apply, but they are based on isolated structural element behaviour (Franssen, *et al.*, 2009). Recent accidental fire and full-scale fire tests which will be described in next section attracted particular interests to assess the global behaviour of the steel structure. For a complete building, each structural element performance relies on the interactions with other members (Wang, 2002). Therefore, to predict more accurate structural response in fire, advanced calculation methods must be involved.

2.1.3 Advanced calculation methods

Advanced calculation methods are sophisticated computer programs that are able to predict realistic fire response of structures. They can be used in modelling from one single element to a complete structure. Generally advanced calculation methods are based on Finite Element Analysis (FEA) and consider material and geometric nonlinearity (Frassen *et al.*, 2009). This allows them to be applied to any type of structure with any kind of fire curve, and simulate complex structural response.

The advanced calculation methods are able to provide accurate predictions which can sometimes be used as substitutions for full-scale fire tests (Wang, 2002). The only disadvantage is that it requires specific user knowledge, and long runtime, so they are not suitable for daily design. Currently, many computer programs have been developed, such as VULCAN (Huang, 2001a), SAFIR (Frassen, 2007), ABAQUS etc which employ advanced calculations. In this research VULCAN is used for the analyses, and is described later.

2.2 Observation of the behaviour of composite floors in fire

2.2.1 Broadgate fire

In 1990, an accidental fire occurred in a 14-storey partly completed steel frame building in the Broadgate development (Lawson *et al.* 1991). The building structure consisted of composite steel beams and concrete slabs with steel decking. It was intended to have a 90 minutes standard fire resistance to the steel structure, but the passive fire protection had not been fully applied at that time and was especially missing on the ground floor which was the floor of origin. It had a sprinkler system but the sprinklers were not in operation because the building was still under construction. The contractor's site office and equipment were located on this floor and the fire started in the contractor's site office. Due to the lack of an active fire protection system, the fire fully developed. It burned severely about four and half hours. It was estimated that the maximum gas temperature reached 1000°C and the maximum steel temperature reached no less than 600°C (Wang *et al.*, 2013).

In terms of the fire performance of the structural elements, the steel beams experienced distortion and local buckling, the steel columns suffered localised failure and axial shortening

(Figure 2-3). It was found that the localised failure within the steel beams and columns were due to restrained thermal expansion (Wang *et al.*, 1995). The structural elements lost their load-carrying capacity and caused extensive vertical displacement to the floor slab. On the other hand, although individual steel elements suffered extensive damage, there was no collapse, the floor slab maintained its integrity and successfully prevented fire spreading to the upper floors. This was attributed to the ability of composite slabs to transfer the load from the failed steel beams to other parts of the structure (Wang *et al.*, 2013).

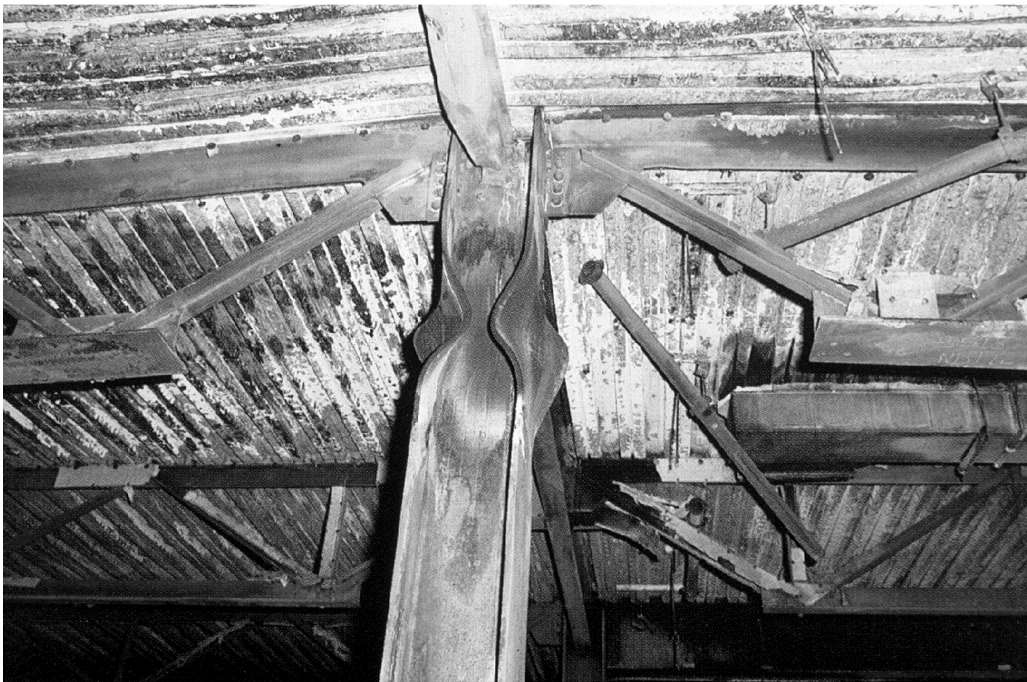


Figure 2-3: Buckled column from the Broadgate fire (Lawson *et al.*, 1991).

The Broadgate fire illustrated that steel framed buildings without passive fire protection to all the main structural elements have the ability to remain stable without collapse during and after severe fires. It showed the possibility of considering the whole structural behaviour instead of testing elements individually in order to reduce fire protection costs by allowing some steel

beams to fail. Therefore, following the Broadgate fire, a series of full-scale steel frame building fire tests were undertaken in Cardington, UK to assess steel structure behaviour in fire conditions.

2.2.1 Cardington full-scale fire tests

Following the Broadgate accidental fire, a fire research programme for fire safety design of steel framed buildings was conducted by the Building Research Establishment (BRE) in UK commencing in 1994. An eight-storey steel-framed composite building was constructed and tested in fire in Cardington (Lennon, 1996). Six fire tests were conducted for different load and support conditions, from a fire test of one restrained steel beam to large compartment fire tests. Within the compartments, some of the perimeter beams and columns were protected but the interior secondary beams were unprotected (Purkiss and Li, 2013). During the fire tests, unprotected steel beam temperatures reached over 1100°C which was significantly higher than the limiting temperature suggested from isolated element analysis, and their strengths had reduced over 95% (Wang *et al.*, 2013). After each fire test, the floors were observed to have experienced extensive deflections which in some cases far exceeded the isolated element deflection criteria, but no collapse occurred (Figure 2-4).



Figure 2-4: Floors experienced large vertical deflections (Newman *et al.*, 2000)

The Cardington full-scale fire tests confirmed that structural members in real steel-frame buildings have significantly greater fire resistance than isolated members in the standard fire tests. This was because in real building fires the fires usually remained localised, structural members were continuous over the floors and restrained by other members, and the heated area received significant restraint from the cooler areas surrounding it (Huang *et al.*, 2001). It was discovered that the tensile membrane action may have occurred as the composite slabs transferred the load from the weakened secondary beams to the edge beams and formed a compression ring around the perimeter and a tension zone in the middle during which the deflection was increasing.

2.3 Tensile Membrane Action

The mechanism of tensile membrane action occurs when the deflection of a slab panel increases, the reinforcement mesh goes into tension, the membrane force in the central region changes from compression to tension. It forms a tension zone in the middle and a compression ring around the perimeter. The loads are supported by the mesh anchored at the supports which have sufficient in-plane restraints such as internal slab panel edge supports under continuous slabs. If the edges do not have enough restraint such as an external edge support, tensile membrane action can still develop by forming a compression ring at the edges (Wang, 2002). As shown in Figure 2-5, tensile membrane action mechanism in a simply supported slab panel (Bailey and Toh, 2007) forms a tension zone in the centre of the slab and a compression ring around its edges. It provides increasing load-carrying capacity for the slab with increasing deflection which elps balance the loss of strength of the floor system components with increasing temperature.

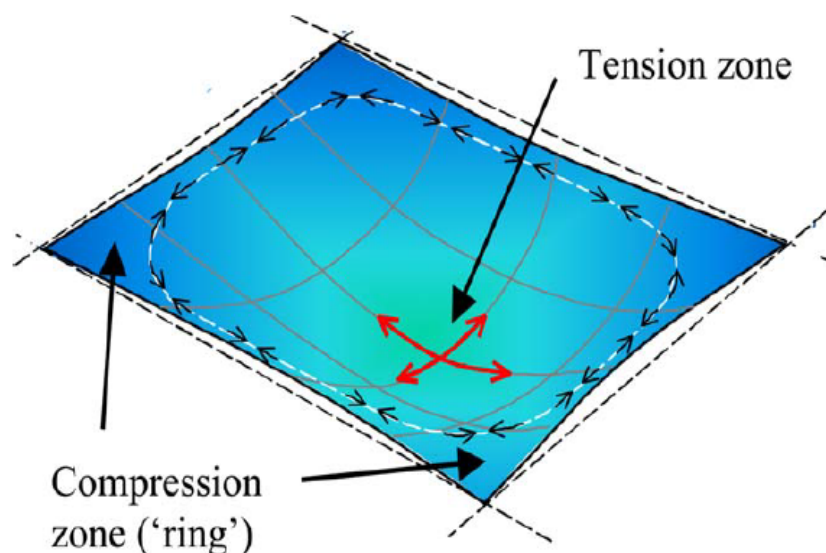


Figure 2-5: Tensile membrane action of a simply supported slab (Bailey and Toh, 2007)

2.3.1 History of Tensile Membrane Action

Before tensile membrane action was discovered, yield-line theory (Johansen, 1963) was investigated as an upper bound approach (Park and Gamble, 2000). Yield-line theory shows that as the load increases to high load level, slabs crack and the tension reinforcing steel within the slabs start yielding at the position with the large deflection. With further loading, the yield lines will be propagated until they separate the slab into segments to form a collapse mechanism (Park and Gamble, 2000). Figure 2-6 shows a typical yield line crack pattern in a simply supported concrete slab (Sawczuk and Winnicki, 1965). The yield lines are the plastic hinge lines that allow the rigid regions to rotate with respect to each other. The rotations occur about the yield lines and also about the edges of the slab. The ultimate load is determined by using the equations of equilibrium (Moy, 1996).

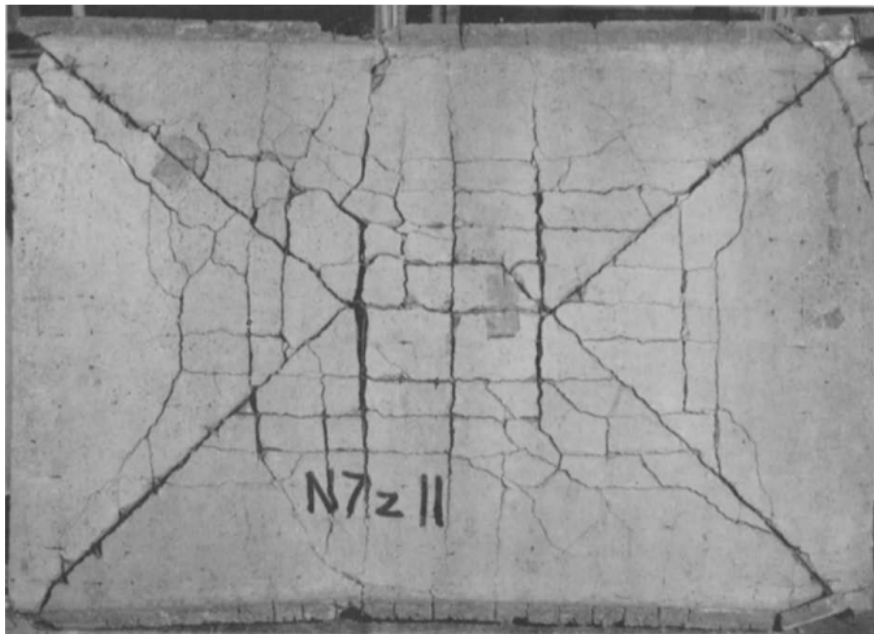


Figure 2-6 : Yield line crack pattern in ambient temperature loading test (Sawczuk & Winnicki, 1965).

However, in concrete slab experiments conducted by Wood (1961) and Powell (1956) it was found that the actual load-carrying capacity of two-way slabs is much higher than that predicted by yield-line theory because of membrane action. Park (1964a; 1964b) confirmed that the yield-line strength of slabs is enhanced significantly by membrane action within the slabs at ambient temperature, but only at large deflections.

Large deflections in floors are not acceptable in ambient temperature structural design, for which the deflection limits associated with yield-line formation are an upper bound. However, it is not necessary to consider deflection limit in fire, as long as integrity failure does not occur. The stable generated large deflections from full-scale fire tests therefore pointed to the use of tensile membrane action as a viable means to enhance load carrying capacity of slabs in fire.

However, it was hard to obtain conclusive evidence directly from the Cardington tests on which to base a design method, due to the inherent complications of conducting full-scale fire tests (Bailey, 2000). Therefore, further tests needed to be undertaken.

2.3.2 BRE Garston ambient temperature concrete slab test

After the Cardington full-scale fire tests, Bailey (2000) suggested to test a simply supported composite slab to confirm the existence of tensile membrane action as the slab had large deformation. Due to the problems of using measuring devices in fire, the test had to be undertaken at ambient temperature (Bailey, 2000).

Under increasing uniform distributed load (UDL) during the test, the concrete slab 'failed' after the formation of a central full depth crack(Figure 2-7), but it did not collapse. This failure was under a load level that was approximately double of the load calculated using the classic yield

line theory. The test demonstrated and confirmed, through observation of the deformation pattern and strains generated in the reinforcement, that tensile membrane action occurred with large displacement and provided significant enhancement in addition to the yield line capacity (Bailey, 2000).



Figure 2-7: Full depth crack forming in the central slab (Bailey, 2000).

Following the test, Bailey developed a simple design method with tensile membrane action called the Bailey-BRE method. This will be introduced in the section 2.4.

2.4 Design methods with Tensile Membrane Action

Accidental fires and full-scale fire tests prove that tensile membrane action is beneficial for the fire resistance of composite steel-concrete floors. Therefore design methods that can provide reasonable predictions of structural fire behaviour including tensile membrane action have been developed for everyday design. This section follows the application of the concept into design practice.

2.4.1 Bailey – BRE method

Bailey (2000, 2001, 2003), Baily and Moore (2000) and Bailey and Toh (2007a, 2007b) initially developed a simplified structural fire design method for composite slabs by using the enhancement of tensile membrane action. Instead of the traditional approach of protecting all exposed steelwork, it divides the composite floor into several rectangular slab panels to design them as whole units. Each slab panel consists of protected edge beams and unprotected interior beams as shown in Figure 2-8. Load is transferred to the increasingly stronger composite slab at large deflections as the unprotected interior beams lose strength and stiffness in conditions.

Two types of edges are at the perimeter of the slab panels depending on the position of the slab panels. The slab panels at the corners or edges of a building do not have lateral restraint over one or two edges; they are called external edges. The lateral restraints to these edges are limited by the stiffness of the building system. The slab panels in the middle of the floor have reinforcement continuous over their edges, called internal edges. The internal edges provide lateral restraints and enhance the stability of the edges and the panels. The Cardington full scale fire tests showed large deformations within slab panels and large cracks at their perimeter (Bailey, 2003a). Therefore, the Bailey-BRE method conservatively assumes no lateral restraints and isolates slab panels with four external edges without considering other support conditions.

The Bailey-BRE method assumes that there is constant vertical support under the edge beams of the slab panel throughout the duration of fire. This is due to the fact that the edge beams are protected and have concrete slab running over them.

The outcome of the Bailey-BRE method is to produce a tensile membrane action enhanced yield-line capacity W_u from the whole slab panel, and compare the W_u with the design load W^* (Wang *et al.*, 2013).

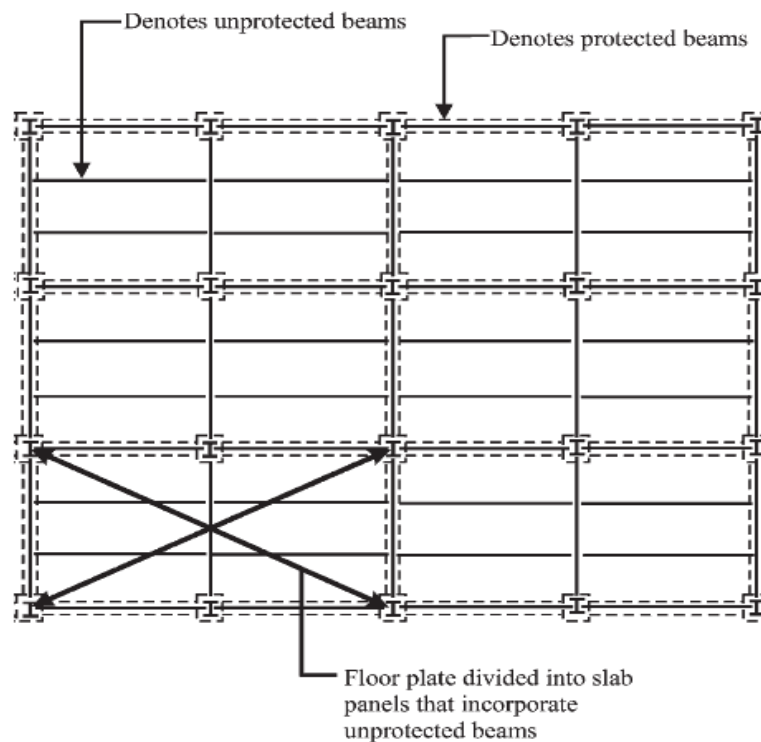


Figure 2-8: Division of floor into slab panels with unprotected beams (Bailey, 2003)

The Bailey-BRE method was initially developed for isotropically reinforced slabs (Bailey, 2000), then extended to allow the specification of orthotropic reinforcement (Bailey, 2003). Further development (Bailey and Toh, 2007a) has been made to refine the in-plane stress distribution, and predict of compression failure. Maximum allowable deflection has been limited in order to avoid integrity failure including full depth crack forming across the shorter span or compression crushing of concrete at the corners of the slab. For slab panels subject to fire, both mechanical strains and thermal bowing effects are considered in the Bailey-BRE method.

The maximum allowable deflection of the slab panel is determined by:

$$v = \frac{\alpha(T_2 - T_1)l^2}{19.2h} + \sqrt{\frac{0.5f_y}{E_{t=20^\circ\text{C}}} \times \frac{3}{8}L^2} \quad \text{Equation – 1}$$

Where v is the maximum allowable deflection that forms the tensile membrane action; α is the coefficient of thermal expansion of concrete; $T_2 - T_1$ is the temperature difference between the top and bottom surface of the slab which is obtained from Cardington fire test data; h is the effective depth of the slab; l and L are the length of the shorter span and longer span of the slab, respectively; f_y is reinforcement yield stress; and E is the elastic modulus of the reinforcement (Bailey, 2003).

2.4.2 The Slab Panel Method (SPM)

2.4.2.1 Introduction

The SPM has been developed since 2001 in New Zealand (Clifton, 2001), with the 2006 version still officially in use (Clifton, 2006), although it has been substantially improve to the 2014 version (Clifton and Abu, 2014). It has been applied to high-rise steel framed buildings in the City of Auckland over the last 6 years. A computer program has now been developed, and the current version of the program is SPM 3.1. Similar to the Bailey-BRE method, it divides the whole floor into several rectangular slab panels (Figure 2-9) and is based on an isolated slab panel but expands it by accounting for reinforcement continuity, edge beam deformation and unprotected secondary load-carrying capacity. It also includes assessment of individual components of slab panels such as protected beam and columns (Wang *et al.*, 2013).

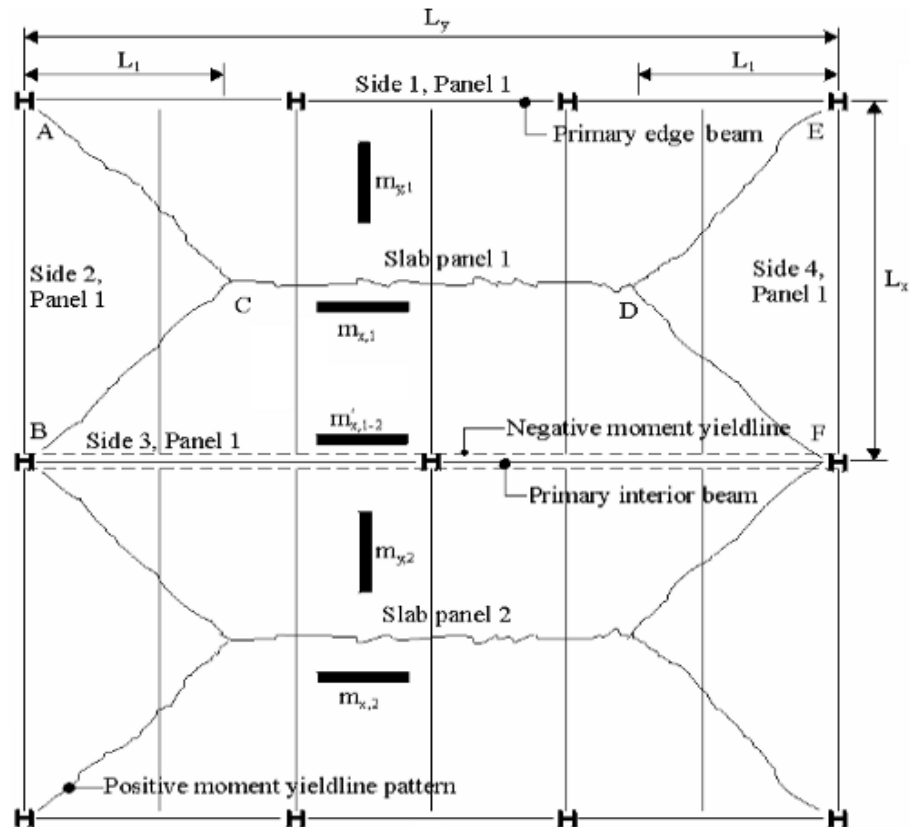


Figure 2-9: Floor plan showing dimensions for yield line pattern and developed moments
(Clifton, 2006)

2.4.2.2 Development work undertaken

After the Cardington full-scale fire tests and the Gaston ambient temperature slab panel test, Bailey (2000a, 2000b) proposed the tensile membrane design concept, HERA developed it into a general design procedure and produced the first edition of SPM in 2001.

Incorporating it with the results of the furnace testing of six slab panels (Lim, 2002), significant improvement of the detailing provisions for dependable inelastic response were made and second edition of SPM was generated. The second edition of SPM improved determination of

slab and reinforcement temperatures, and revised reinforcement limits for integrity (Mago and Clifton, 2003).

Finite Element Analysis (FEA) for six slab panel fire tests was undertaken (Lim *et al.*, 2004) by using FEA software SAFIR (Frassen, 2007). The analysis confirmed that tensile membrane action occurred and enhanced the yield-line capacity in fire.

Another modelling of three UK bare steel and composite standard fire test was undertaken by Mago (2004). It was proved that SPM is inclusion of the unprotected interior secondary beam into the slab panel load-carrying capacity is valid. The research also showed that the distribution of loads to the edge beams as followed the yield line pattern (Clifton 2006).

Based on the deflection-time curve of the slab panel fire tests and FE analyses, Clifton (2006) found that the deflection of slab panel in fire is not dependent on the time of standard fire exposure. For example, Figure 2-10 demonstrates a typical deflection curve of a FE modelled slab panel under standard fire exposure. The slab panel deflection behaviour can be categorised into three stages (Clifton, 2006). At stage one, the deflection increases quickly with increasing time, but the rate of deflection decreases. At stage two, the deflection linearly increases along time with constant rate. At the third stage, the slab panel is in its pre-failure stage, the deflection nonlinearly increases with increasing rate of deflection. The design objective of SPM is to keep the slab panel in stage two within the required fire resistance rating. Therefore, Clifton (2006) developed a modification factor C_{iso} to the deflection limit Δ_{limit} as a function of the structural fire severity.

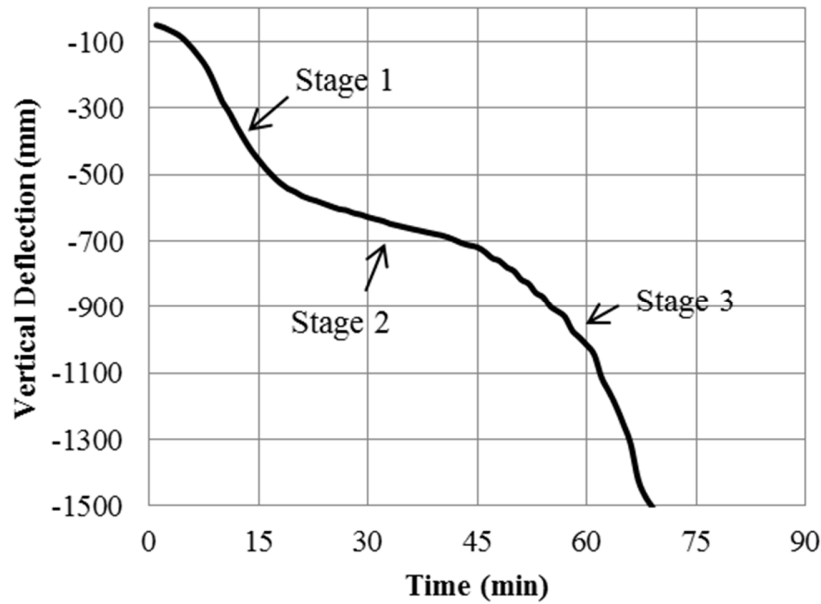


Figure 2-10: Three stages of deflection in fire

The edge beam deflection, unprotected secondary beams contribution and the modification factor C_{iso} have been included into the third version of SPM. Currently, ongoing research and feedback is still being undertaking in order to develop SPM to provide dependable use of unprotected steel members in steel-concrete composite floor systems.

2.5 The VULCAN FINITE ELEMENT PACKAGE

In this research, FEA computer program VULCAN is used as an advanced calculation method for the design of composite floor. VULCAN (Huang *et al.*, 1999, 2000, 2003a, 2003b; Huang, 2010) has been developed at the University for Sheffield as a specialist program for steel and composite buildings in fire conditions. It is able to model the structural fire behaviour of steel composite buildings in three-dimensions as shown in Figure 2-11. VULCAN has been widely validated in previous research (Huang *et al.*, 2002) with Cardington full-scale fire tests. The research indicated that VULCAN predicts structural behaviour of composite and steel frame

building with good accuracy. It is attributed to the robust thermal and structural analysis model embedded within VULCAN.

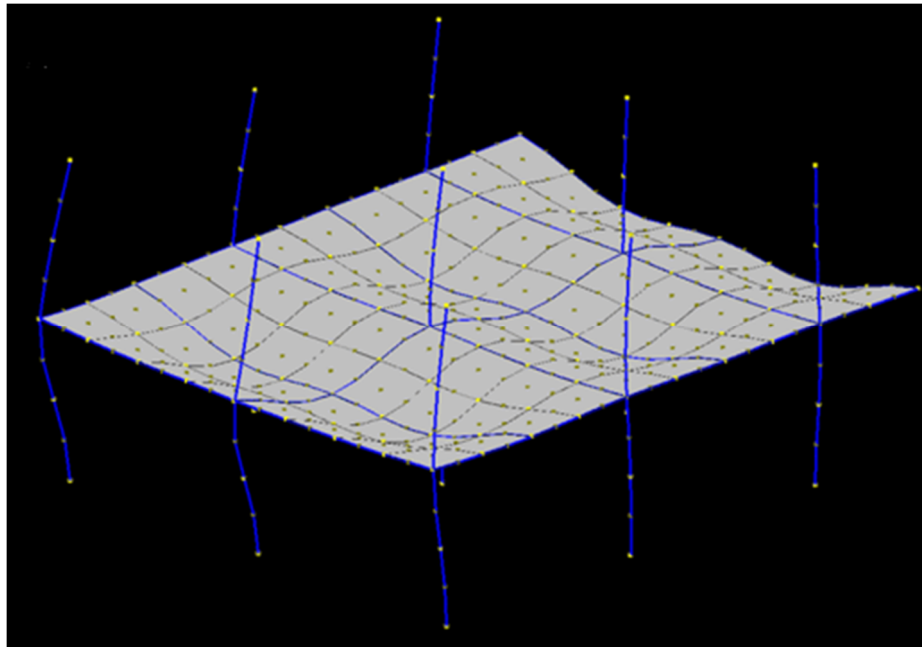


Figure 2-11: Vulcan can model the structural fire behavior in 3D, from vulcan-solution.com

To model structures subjected to fire, the temperature change within the structural components must be analysed first because structural fire behaviour is dependent on the temperature variation. VULCAN allows the user to specify the temperature-time fire curve to apply to the components and perform a thermal analysis.

For analysis of the reinforced concrete slab, VULCAN uses an approach called nonlinear layered procedure which is based on Mindlin/Reissner (thick plate) theory (Huang *et al.*, 2010). Both geometric and material non-linearities are taken into account. The approach divides the reinforced concrete slab floor into layers. Each layer is assumed to have uniform temperatures, but can have different temperatures between layers (Huang, 2003a). The two direction

reinforcements are treated as smeared concrete layers of thin sheets of steel within the thickness of the slab as shown in Figure 2-12.

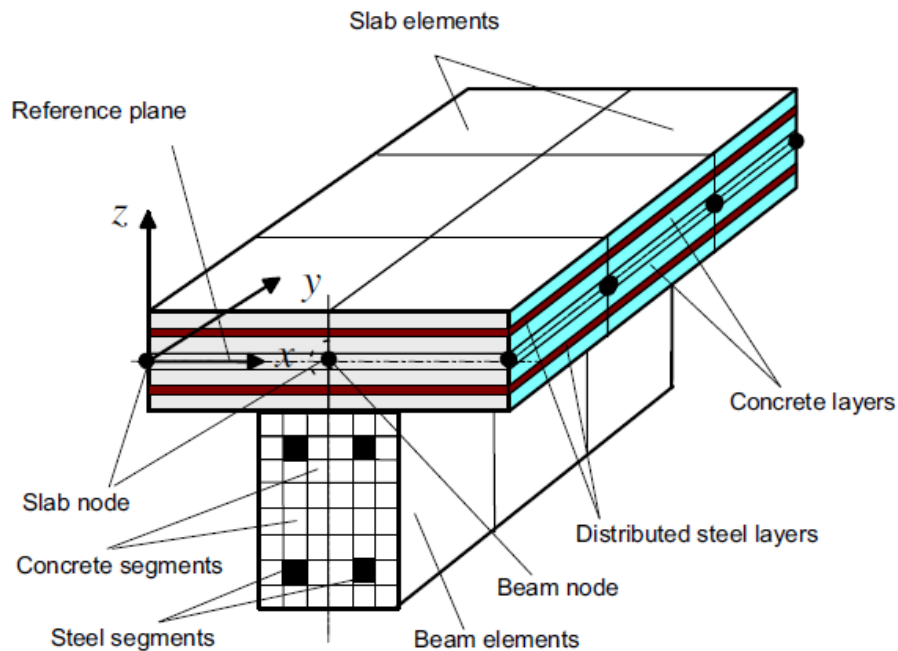


Figure 2-12: Slab and beam elements in VULCAN (Huang, 2010)

Trapezoidal composite slab consists of an isotropic upper continuous slab and an orthotropic part in one direction as shown in Figure 2-13. When performing thermal analysis on the concrete slab in VULCAN, the trapezoidal profile needs to be transformed to an equivalent solid slab. Three thermal analysis methods are available for the transformation process. They are Thin Continuous concrete Topping (TCT), Effective Stiffness (ES), and Effective Depth (ED). They can all be used in VULCAN. An explanation of the implication of using each of these is given below.

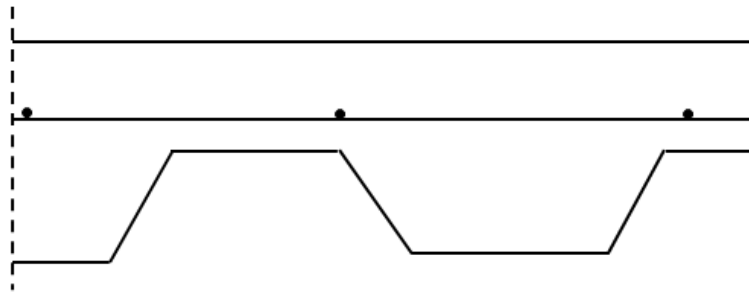


Figure 2-13: Trapezoidal composite slab profile

The TCT method only models the thickness of upper continuous concrete part, it is assumed to be directly exposed to fire as it is the shallower parts of a composite deck. This method produces relatively high reinforcement temperatures. The ES method models the full depth of the slab. It accounts for the orthotropic lower portion of the slab by calculating effective stiffness factors α_x and α_y for bending in two directions. Detail of this method is described by Huang (2000). The ED method is from Eurocode 4 (CEN, 2005) and it is currently commonly used. It transfers orthotropic composite slabs into an equivalent solid slab with an average depth that is thinner than the ES method but thicker than the TCT method. Figure 2-14 demonstrates the ES, ED and TCT method in composite beam cross section, respectively.

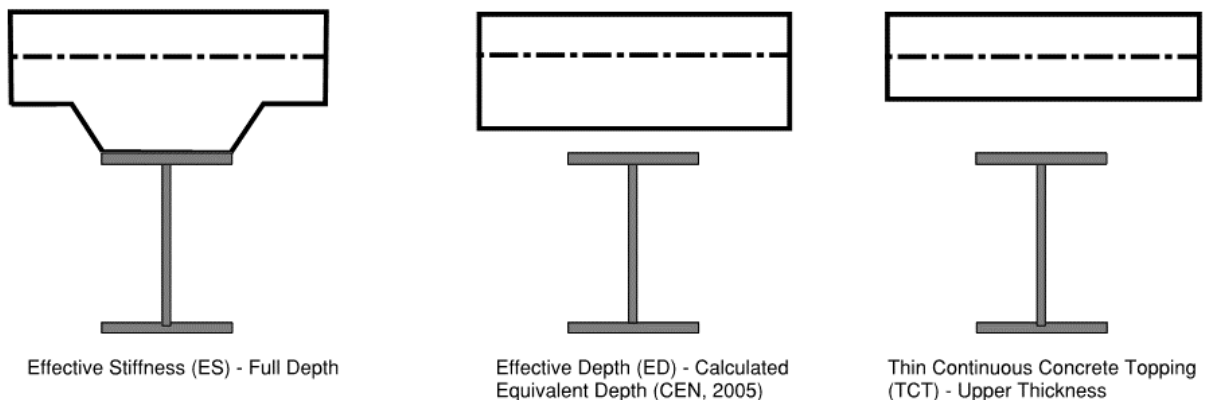


Figure 2-14: VULCAN Thermal Analysis Methods

The thermal properties of the steel and concrete from Eurocode2 (CEN, 2004) are adopted in the model, they change with elevated temperature. The model also accounts for the influence of moisture initially held within the concrete and protection materials. Huang (2010) recently modified the model to account for the effect of concrete spalling on the concrete members.

To perform structural analysis of the frame elements including beam or column, VULCAN accounts for the geometric and material nonlinearities. It divides the cross section of beam-column into a matrix of segments and each segment can have different material and thermal properties (Huang *et al.*, 2009).

In structural analysis, VULCAN accounts for the complication of structural fire behaviour such as stress-strain degradation, thermal expansion, cracking and crushing of concrete slabs, and yielding of reinforcements (Huang, 2010). This makes VULCAN to be capable of modelling composite steel-concrete floors at elevated temperature incorporating with membrane actions. Detailed descriptions of the formulation in VULCAN modelling are presented by Huang *et al.* (2003a, 2003b).

In VULCAN, a composite steel-frame building can be built as an assembly of finite beam column and slab elements. All the elements are constructed by nodes. The slab elements and beam-column elements are constructed with nine-node shell elements and three-node frame elements, respectively. The smeared crack model is adopted in VULCAN for modelling cracking of concrete slab (Huang, 2003a). In the smeared crack model, crack in the slabs are assumed spread within a whole grid surface once any crack occurs. For example, if a VULCAN modelled slab panel uses 1.5 m × 1.5 m grid size, VULCAN assumes an entire grid fails once any crack occurs on that grid. Therefore, the grid size of the slab and beam elements VULCAN determines

the accuracy of the result and duration of runtime. In this research, grid size of 1 m × 1 m is used for accuracy and reasonable runtime. The validation of grid sizes will be covered in Section 3.3.2.

It is assumed that the nodes of beam-columns and slab elements share a common plane called plane of reference (Huang *et al.*, 2009), as shown in Figure 2-12. The plane of reference is at the middle of the thickness of the concrete slab, so the beam under the concrete slab can be determined by defining the distance from the middle of the concrete slab to the middle of the beam.

Boundary conditions are significant in modelling the global behaviour of structures. Six degrees of freedom (both translation and rotation in three directions) are allowed in VULCAN.

2.6 Limitation of the Simple Methods

Recent research (Abu, 2009; Abu and Burgess, 2010; Abu *et al.*, 2010, 2011) developed a collapse mechanism that focuses on the edge beam failure while using the tensile membrane action method. The failed edge beam of a slab panel will cause a folding mechanism leading to slab integrity failure as shown in Figure 2-15.

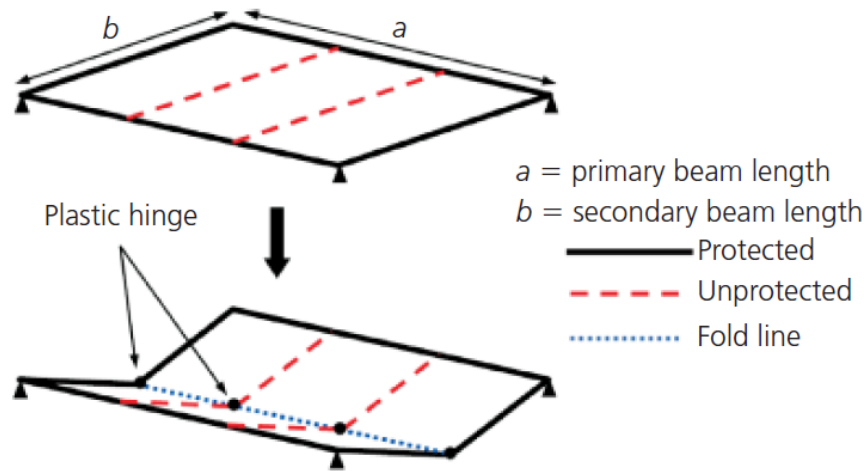


Figure 2-15: Slab panel folding mechanism (Abu *et al.*, 2012)

Abu *et al* (2012) have shown that the assumption of constant vertical support around the edges of slab panel was not sufficiently conservative and would cause premature failure of the slab panel by a series comparisons between the Bailey-BRE method predicted deflection and VULCAN modelled results. It was found that the edge beams must function as effective stiff supports in order to generate the two way tensile membrane action. If these beams form plastic hinges, the slab panel load carrying capacity significantly reduces as the entire panel undergoes a plastic collapse mechanism (Abu *et al*, 2012).

Furthermore, different slab panel sizes and reinforcement arrangement also influence the predictions (Bailey, 2003b). To follow the Bailey-BRE method, a slab panel's edge beams needs to be protected to ensure the constant stiff vertical support. In reality, the edge beams would always deflect, and this may cause a premature edge beam failure of the slab panel if the deflection is more than critical. Results obtained from the Bailey-BRE method show that the

method accurately predicts internal slab panel behaviour, since the continuous sides enhance the vertical edge supports (Abu *et al.*, 2008).

2.7 Impetus of the current research

In conclusion, this chapter covers the background literature of this research, as follows:

- The FRR required for the structural members are determined by the fire engineers. It is based on the building's fire safety features.
- Structural fire design considers the load-carrying capacity of the structural members, which is similar to the ambient temperature design.
- Traditional design method only considers structural member's performances.
- Previous accidental fires and full scale fire tests shows that tensile membrane action can be used in fire design by considering a whole slab panel's fire resistance.
- Finite Element Analysis (FEA) package VULCAN simulates the interaction between structural members in fire and takes account tensile membrane action. However it is time-consuming and requires specific user knowledge.
- The SPM, as a simplified design method incorporating tensile membrane action is based on isolated slab panel.
- The SPM incorporates certain deflection and negative moment capacity at slab panel protected internal edges. The suitability of SPM for modeling continuous slab panels needs to be ascertained.

This research therefore seeks to quantify the effectiveness of edge-beam support in the SPM, especially where continuity is concerned.

3 METHODOLOGY

Introduction

This chapter presents the methodology used for this research. It firstly introduces the physical properties of the modelled composite floor. Then it describes how the floor was built in both VULCAN and the SPM, justifying the selection of various input parameters. Finally it outlines the steps used in the comparison in subsequent chapters.

3.1 Floor Description

Before using the SPM and VULCAN in structural fire design, the ambient temperature property of the structural components of the floors such as the beam size, spacing, slab depth, concrete strength etc must be known beforehand.

The slab panels selected in this research follow recommendations of a design guide known as SCI P-288 (Newman *et al.*, 2006). SCI P-288 was developed by the Steel Construction Institute (SCI) to design steel frame buildings using tensile membrane action (Abu *et al.*, 2007). It provides the required design data for slab panels for the required fire resistance time. It consists of various slab panel arrangements and required reinforcement mesh sizes for a specified times of fire resistance (Abu *et al.*, 2007).

In previous research, Abu *et al.*(2012) investigated the accuracy of the Baily-BRE method by comparing results of three slab panel sizes with VULCAN structural analysis. ComFlor 60 decking (Figure 3-1) was used. In this research, as the SPM is similar to the Bailey-BRE method. The

same slab panels with 9 m × 9 m, 9 m × 6 m and 9 m × 12 m with 130 mm deep trapezoidal profile floors are chosen for the comparison.

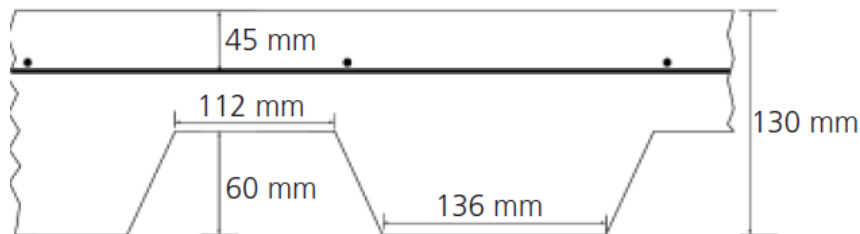


Figure 3-1: Concrete trapezoidal slab profile (Abu *et al.*, 2012)

Initially, the 9 m × 9 m slab panel, as shown in Figure 3-2, was modelled in VULCAN and SPM. The solid lines show the protected edge beams while the dashed lines represent the unprotected secondary beams. The steel beams are designed according to NZS 3404 (SNZ, 2007) with loads used for ‘office’ usage in accordance with NZS 1170.1 (SNZ, 2005).

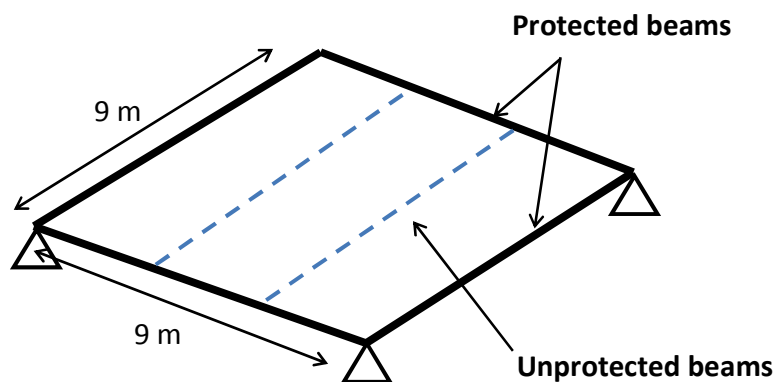


Figure 3-2: 9 m × 9 m isolated slab panel with protected and unprotected steel beams (Gu *et al.*, 2013)

For high rise office buildings, at least 60 minutes fire resistance rating is required for occupants to safely evacuate and prevent structural collapse. Therefore, the slab panel is designed for 60

minutes of fire resistance. The analyse are set up for a duration of 90 minutes of exposure to the standard ISO834 fire exposure in order to investigate slab panel failure behaviour.

In the previous research (Abu, 2007; Abu, 2008; Abu *et al.*,2012), the concrete cube strength (fcu)40MPa was used as it is the British concrete property and used in Bailey-BRE method. However, New Zealand concrete has 30MPa cylinder strength (f'_c) and this is used in the SPM. The two concretes have very similar compression strength, as the raio of cylinder/cube strength for normal weigh or structural lightweight concrete is 0.85, meaning the fcu = 40MPa UK concrete has a cylinder strength of 32 MPa. Therefore 30MPa cylinder strength is used as the SPM is investigated in this research. Reinforcing mesh A193 is used, which is consistent with the research by Abu *et al.*(2012). According to SCI P-288, A193 is the minimum size of reinforcement required for 60 minutes fire resistance rating of a 9m x 9m slab panel. It has 7 mm diameter bars with 500 MPa yield strength at 200 mm spacing.

The design loads consist of the slab panel's self-weight, G, and office live load, Q, as shown in Table 3-1.

Table 3-1: Design Loading

Dead Load	kN/m²
Slab self-weight	3.12
Beam self-weight	0.13
Mesh (A193)	0.03
Live Load	
Office usage	3.00

Load combinations, $1.2G + 1.5Q$ for Ultimate Limit State (ULS) and $1.0G + 0.4Q$ for Service Limit State (SLS), were used in accordance with NZS 1170.1 (SNZ, 2005). In accordance with NZS3404 (SNZ, 1997) structural steel design standard, steel beam sizes 460UB82.1 and 310UB40.4 were adopted as primary and secondary beams, respectively. A generic fire protection scheme was applied on the designed slab panel. The temperatures of the protected primary and edge secondary beams were limited to 550°C at 60 minutes of standard fire exposure. To achieve this, fire resisting gypsum boards (density = 800 kg/m^3 , specific heat capacity = 1700 J/kg/K , conductivity = 0.2 W/mK) were used.

The slab panels are modelled in SPM and VULCAN, where thermal and structural analyses are required to be undertaken for both software. The SPM computer software normally only provides the results at certain times of fire severity by simply inputting the required values. It does not show the procedure and relationships between the temperature and structural response. In order to investigate the slab behaviour and compare the results at each time step with VULCAN, a spreadsheet was used to calculate the SPM steps outlined in HERA Report R4 - 131 (Clifton, 2006).

In VULCAN, thermal analysis of the concrete slab was conducted with the use of the finite element software ABAQUS (ABAQUS, 2010) while steel beam temperatures were calculated by the lumped mass approach in Eurocode 3 (CEN, 2005). The temperatures were then entered into VULCAN for the structural analysis.

3.2 The Slab Panel Method (SPM) Setup

The SPM setup in this research is based on the third edition of the SPM. The detailed procedure is described in HERA Report R4-131 (Clifton, 2006).

3.2.1 The SPM Thermal Analysis

The SPM provides equations and tables for users to determine the reinforcement temperature, secondary steel beam temperature and the concrete slab temperature.

3.2.1.1 Reinforcement temperature

The first step is to determine the reinforcement temperature in order to obtain the change in reinforcement yield strength during the standard fire exposure.

The SPM divides reinforcement into general and interior reinforcement. General reinforcement is within one slab panel. As the slab panel deforms in fire, they provide slab panel positive moment capacity. On the other hand, interior reinforcement is located at the edge between slab panels and generate negative moment capacity at the edge in fire.

The SPM takes both general and interior reinforcement temperatures into account. The reinforcement temperatures are obtained from the equations in HERA Report R4-131 (Clifton, 2006). HERA Report R4-131 has provided equations for various slab profiles including trapezoidal decking, flat slab and clipped pan decking. Only trapezoidal decking has been investigated. Figure 3-3 shows a cross-section of a trapezoidal concrete slab consisting of reinforcing meshes in two directions. The x-direction reinforcing bars are below the y-direction reinforcing bars.

An important step is to determine the heat flow path from the bottom to the reinforcement mesh position within the decking. As a result of the shape of the trapezoidal deck, the temperature of the reinforcements are not constant along their directions. In SPM, the heat flow path is determined by three distances, u_1 , u_2 , and u_3 above the rib, as shown in Figure 3-3.

Figure 3-4 shows the predicted reinforcement temperatures of each direction against time.

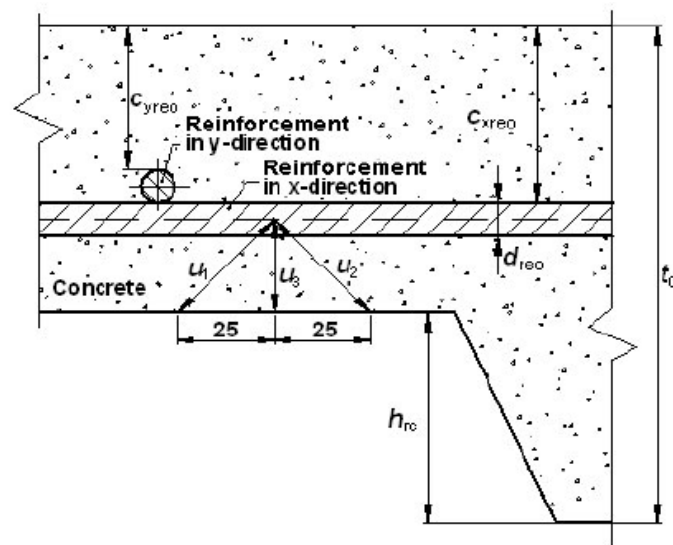


Figure 3-3: Mesh position and heat flow path for mesh temperature distribution (Clifton, 2006).

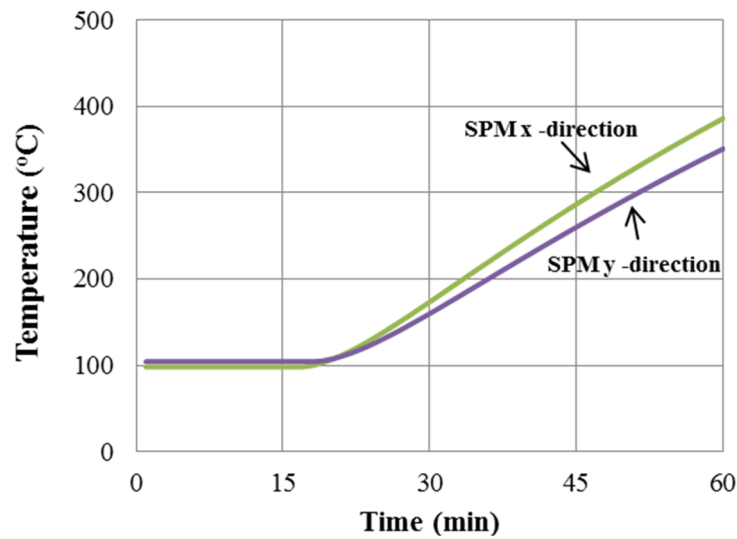


Figure 3-4: SPM predicted temperature against time

Not only has the general reinforcement temperature calculation within the concrete slab, SPM also provides the temperature calculations for the interior reinforcement. The method of calculating the interior reinforcement temperature is the same as that for the general reinforcement. The only difference from the general reinforcement is the interior reinforcement's position above the slab soffit is slightly higher.

3.2.1.2 Concrete Slab Temperature

The next step is to determine the concrete slab's temperature. The concrete maximum temperature has been determined from numerous previous FEA analyses and results from experimental fire tests (Clifton, 2006). The temperatures are categorized by Fire Hazard Category (FHC), which has been used for determining the design fire load energy for buildings of different usages. In this research, office usage is FHC2. For Normal Weight Concrete (NWC)

trapezoidal profile, SPM determines the temperature across top of ribs and average temperature over full deck width are both 750°C (Clifton, 2006).

However, the building usage is not categorized in FHC in the New Zealand Building Code compliance document after 2012. The current version of the SPM still use FHC to define the concrete slab temperature, so users have to check the FHC in the Acceptable Solution (C/AS1).

3.2.1.3 Steel Beams Temperature

As mentioned in Chapter 2, the effect of unprotected steel beams has been taken into account in SPM. The temperatures of the top flange web and secondary beams elements including top and bottom flanges and webs are addressed separately. In SPM, the unprotected steel beams are assumed to be directly exposed to fire and reach very high temperature. The temperature of the top, bottom and web of the steel beams are approximated by 95% of the peak fire temperature (Clifton, 2006). The temperatures of each component are shown in Table 3-2 below (Wu & Li, 2012). As mentioned previously, in estimating concrete slab temperature, slab panels used is FHC2, NWC, therefore the bottom flange, web and top flange are 850°C, 800°C and 750°C, respectively as highlighted below.

Table 3-2: Design temperatures of unprotected secondary beam elements (Clifton, 2006)

	Bottom Flange (°C)	Web (°C)	Top Flange (°C)
FHC1,NWC	750	750	650
FHC2,NWC	850	800	750
FHC3,NWC	900	850	800
FHC1,LWC	850	850	750
FHC2,LWC	1000	950	900
FHC3,LWC	1050	1000	950

3.2.2 SPM structural analysis

3.2.2.1 Design Yield Stress in Elevated Temperature

SPM structural analysis calculates the design yield stress of each element at elevated temperature, and then calculates the bending effect and membrane action within the whole slab panel, since structural members in slab panel act compositely. After temperatures of each structural component such as reinforcement, unprotected steel beams has been obtained, the reduced yield stress of each component in elevated temperature is calculated.

For the cold-worked reinforcement mesh A193 used in the 9 m × 9 m slab panel, SPM utilises the relationships between ambient temperature yield stress $f_{yr\theta}$ and elevated temperature yield stress f_{yr20} given by EC2 (CEN, 2004).

For unprotected secondary steel beams, the relationship of yield stress at elevated temperature from EC 3 (CEN, 2005) is used. Corresponding with the maximum temperature provided in Table 3-2, SPM directly provides the relationship between the ambient temperature

yield stress $f_{ysb\theta}$ and elevated temperature f_{ysb20} for unprotected secondary beams, as shown in Table 3-3 below:

Table 3-3: Relationship between $f_{ysb\theta}$ and f_{ysb20} for unprotected secondary beams (Clifton, 2006)

	Bottom Flange (°C)	Web (°C)	Top Flange (°C)
FHC1,NWC	0.17	0.17	0.25
FHC2,NWC	0.085	0.11	0.17
FHC3,NWC	0.06	0.085	0.11
FHC1,LWC	0.06	0.06	0.17
FHC2,LWC	0.04	0.05	0.06
FHC3,LWC	0.03	0.04	0.05

The $\frac{f_{ysb\theta}}{f_{ysb20}}$ of the bottom flange, web and top flange of unprotected secondary beams are 0.085, 0.11 and 0.17, respectively as highlighted in the Table 3-3.

3.2.2.2 Calculate Positive and Negative Moment Capacity

The next step is to calculate the moment capacity of the slab panel. The moment capacities of the slab panel in the SPM includes the internal tension forces from the reinforcement, and unprotected steel beams which were calculated from the steps above.

As slab panels experience two - way bending, the positive moments in x -direction, m_x and y - direction m_y need to be calculated.

The positive moment in x-direction is determined by the reinforcement in x-direction and unprotected secondary beams. Figure 3-5 shows the development of positive moment capacity.

As it shown in Figure 3-5, the reinforcement in x-direction and the unprotected steel beams provide internal tension capacity during the downwards deflection of the slab panel in fire.

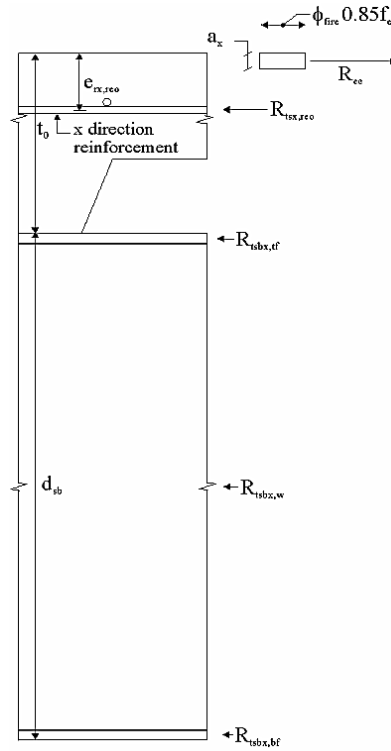


Figure 3-5: Development of positive moment capacity in x-direction by unprotected secondary beams and reinforcement (Clifton, 2006)

The SPM allows user to change the support conditions for each side of the slab panel to determine the edges to be internal or external. Two types of edges may occur at the perimeter of the slab panels depending on the position of the slab panels in the building. As shown in Figure 3-6, the edge at Side 1 of Panel 1 does not have lateral restraint. This kind of edge is called external edge. While internal edges are those in the middle of the floor and have reinforcement continuously over them, such as one at Side 3 of Panel 1 in Figure 3-6. The internal edges provide lateral restraints and enhance the stability of the edges and the panels.

Therefore, the SPM also takes the negative moment capacity in x direction m'_x , which is generated from the slab panel's internal edges into account.

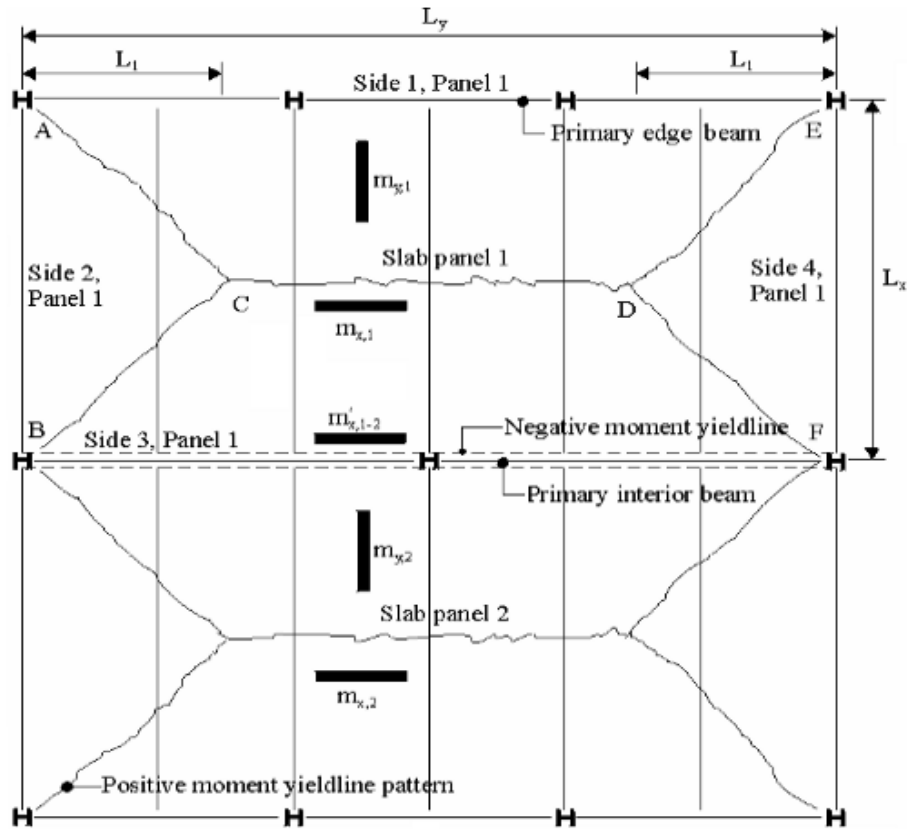


Figure 3-6: Floor plan showing external and internal edges (Clifton, 2006)

3.2.2.3 Determine the Tensile Membrane Enhanced Yield-line Capacity

After obtaining the positive and negative moment capacities, the slab panel's yield – line load – carrying capacity w_{ylo} can be obtained. It is obtained from the yieldline equation for a general rectangular slab with either pinned or fixed edge supports (Park, 1970).

After obtaining the yield-line capacity of the slab panel, the enhancement factor of tensile membrane action is calculated. As mentioned in Section 2.3, tensile membrane action is

produced as the deflection increases during fire. Similar as the Bailey-BRE method, the SPM uses the limiting deflection to determine the tensile membrane action enhancement factor. However, they are modified according to FEA analysis and fire tests (Lim, 2002).

Finally, the SPM calculates the tensile membrane enhancement, e . The equations are taken from Bailey and Toh (2007a). Then the design tensile membrane enhanced load carrying capacity, w_u is checked against the design load, w^* .

The above steps are undertaken for the SPM modeled slab panels. In this research, the SPM models need to be compared with VULCAN deflections. Therefore after the SPM thermal and structural analysis, VULCAN thermal and structural analysis is required to simulate structural response.

3.3 VULCAN Analysis

3.3.1 VULCAN Thermal Analysis

VULCAN traces the structural response of the slab panel throughout fire. It requires users to manually input each structural element's temperature variation throughout the time of the entire modelling. The elements' temperature curves must be obtained before inputting them into VULCAN.

In the same manner as for the SPM, VULCAN thermal analysis procedure can be divided into several components, including the concrete slab, protected primary and secondary beams and unprotected secondary beams.

In this research, the temperature of the steel beams was assumed to be uniform through the cross-section. The equations for calculating the temperature per unit length in Eurocode 3 (CEN, 2005) were used for the unprotected and protected steel beams.

Figure 3-7 shows the temperature curves of the unprotected and protected beams under 90 minutes standard fire exposure. The unprotected beams temperature rises rapidly in the first 15 minutes and then reaches the same temperature as standard fire, whilst the protected beam temperature grows steadily and is limited to below 550°C at 60 minutes as designed.

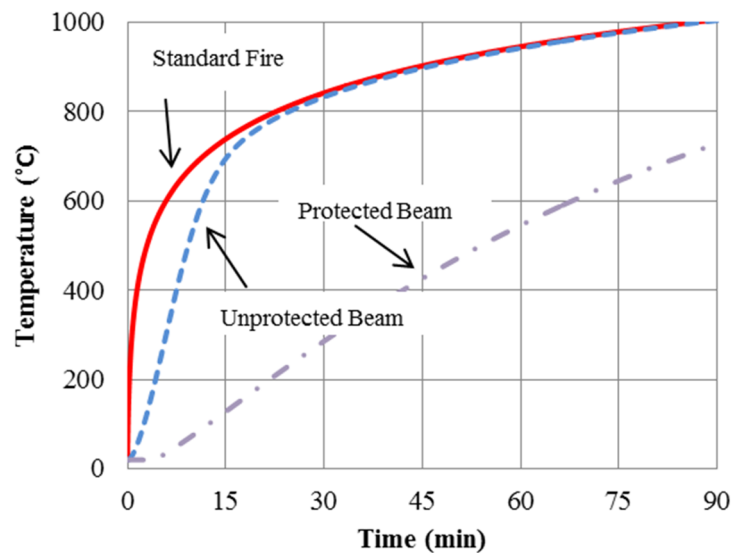


Figure 3-7: Unprotected and protected steel beams under standard fire exposure

For concrete slabs, given the assumption of uniform temperature distribution along the slabs, one-dimensional (1-D) thermal analysis has been conducted in this research. As mentioned in Chapter 2, the cross-section of concrete slab is divided into several concrete smeared layers. However, the trapezoidal slab profile is non-uniform. It consists of a continuous upper part and discontinuous corrugated lower part; therefore it was firstly needed to be transferred to an

equivalent rectangular cross-section slab in order to be thermally analysed. As shown in Figure 2-14, Effective Stiffness (ES), Effective Depth (ED), and Thin Continuous concrete Topping (TCT) methods are available to use in the transformation process. ES uses the full depth of the slab; TCT only uses the thickness of the continuous upper part; and ED uses a calculated average depth in accordance with Eurocode 4 Annex D (CEN, 2005). According to the ED, ES and TCT models, different equivalent thickness of the designed trapezoidal slab were obtained, as shown in the Table 3-4 below.

Table 3-4: Calculated thickness from ES, ED and TCT

	Effective Stiffness (ES)	Effective Depth (ED)	Thin Continuous concrete Topping (TCT)
Thickness(mm)	130 mm	102 mm	50 mm

As mentioned above, the slab is divided into several smeared concrete layers, the temperature within each layer are uniform along the slab, but different from others (Huang *et al.*, 2003a). FPRCBC-T (Huang *et al.*, 1996), which is a thermal analysis computer program to calculate concrete temperature for composite floor was used initially to determine the temperature of concrete slab.

Since this research is to compare the results between the SPM and VULCAN, it is important to confirm that the models are comparative to each other within each step. In the VULCAN thermal analysis, the temperature data obtained and input in VULCAN structural analysis afterwards must be close to the temperature calculated by SPM.

SPM provides equations for calculating the reinforcement temperature, but no equations for concrete slab temperature against time, only temperatures of two directions of reinforcement from SPM can be used to compare with the results from FPRCBC-T. As it can be seen in Figure 3-8, there is a gradual increase of differences between the two directions of reinforcement. This is because SPM uses equations that take account the value of the exact position of reinforcement in each direction. Whereas in VULCAN, the concrete slab was divided into several layers, the reinforcement was transferred into very thin concrete smear layers, so the reinforcement temperature obtained are almost same between the two directions.

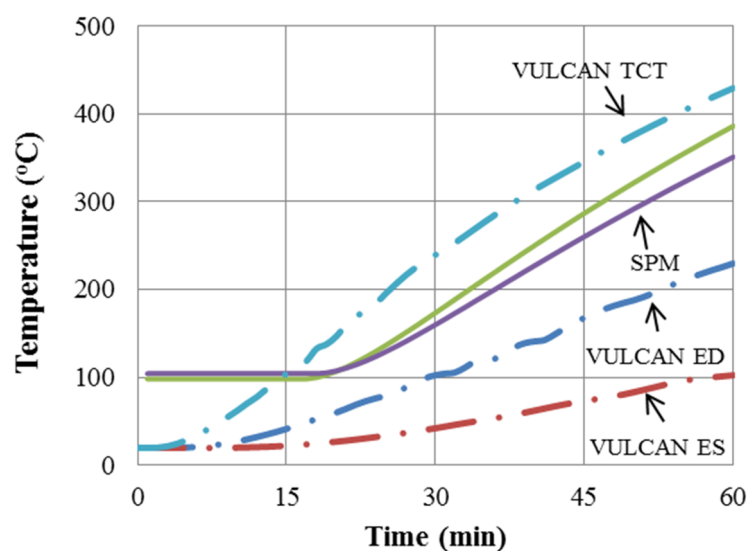


Figure 3-8: Comparisons between the FPRCBC-T results and SPM

As shown in Figure 3-8, throughout 60 minutes exposure to standard fire, ES predicts the lowest temperature as it uses thickest cross-section depth. The temperature obtained from ED method is higher than that from ES, but is much lower than the value from TCT. TCT method provides the highest temperature with time as it uses the smallest cross-section depth. All these temperature – time curves obtained from VUCLAN Thermal are beyond SPM's calculated

temperature. Therefore these temperature curves are not suitable to use in VULCAN for comparison of SPM with Vulcan. It was found due to the fact that European concrete properties embedded within VUCLAN Thermal are different from those in NZ concrete used in SPM. NZ concrete thermal properties need to be used. However, it was not possible to change the concrete properties in FPRCBC-T, as it does not allow the user to specify material thermal properties.

In order to obtain valid temperature input for VULCAN, 1-D thermal analysis was undertaken via ABAQUS (ABAQUS, 2010) because it allows users to specify the material properties. By inputting the NZ concrete properties from Wade (1993), the temperature curves obtained from ABAQUS is different from FPRCBC-T results. They are compared with SPM temperature, as shown in Figure 3-9. The comparison shows that the temperature curve obtained from ED gives the best agreement with the SPM temperature among these three methods, although it gives slightly lower temperature than SPM after 40 minutes. Therefore, temperature from ED was considered to be appropriate to be adopted in the VULCAN structural analysis.

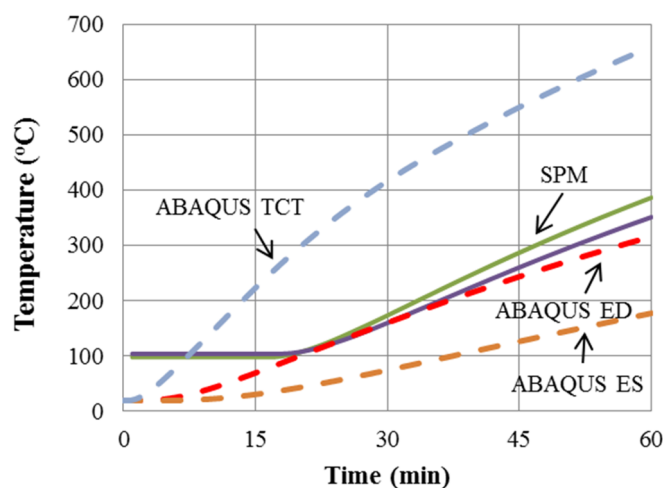


Figure 3-9: Comparisons between the results from ABAQUS Thermal and SPM

Figure 3-10 illustrates the transformed slab cross-section equivalent effective depth and its layers with their corresponding temperature.

Figure 3-10(a) shows that the cross section is divided into 13 layers, and (b) shows the corresponding temperature of each layer. These temperature curves indicate that the higher temperature the layer has, the lower it locates, as the bottom surface of the floor is exposed to fire.

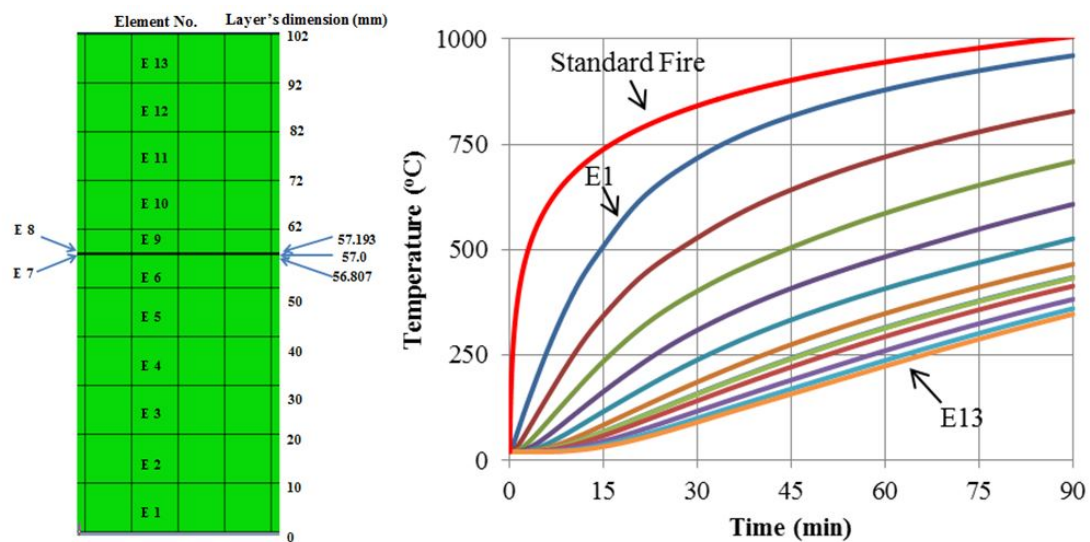


Figure 3-10: (a) Cross-section with layers (left) and (b) temperature curves of the layers (right)

After obtaining the temperature curves of structural members in VULCAN and the SPM, VULCAN structural analysis was undertaken to investigate their corresponding structural response. SPM uses equations to determine the maximum moment capacity and the limiting deflection of slab panel at a specific duration of time equivalent structural fire severity, while VULCAN provides slab panel deflection-time history throughout the model based on the given temperature data.

3.3.2 VULCAN Structural Analysis

To perform structural analysis, VULCAN requires users to input the dimensions of the structural members, temperature data within each structural member. As mentioned in Section 3.1, the concrete slab has a thickness of 130mm with A193 reinforcement. The primary and secondary beam sizes were 460UB82.1 and 310UB40.4. The dimensions of these structural members were input into VULCAN.

Temperature data were obtained through the thermal analysis which was undertaken by using ABAQUS for concrete slab and Eurocode 2 (CEN,2004) and Eurocode 3 (CEN, 2005) equations for protected and unprotected beams, as described in Section 3.3.1. Those temperature data was input into VUCLAN software for the structural analysis.

After inputting the structural and thermal data, VULCAN model would be ready to start simulation. However, it is important to validate the VULCAN model before simulating the slab panel models in this research. This is to confirm whether it is suitable to model the slab panel and compare with the SPM.

3.3.2.1 Validation – BRE Garston ambient temperature test

As mentioned in Chapter 2, VULCAN is well – validated by comparing with previous full – scale fire tests’ results. However, previous full – scale fire tests were only conducted with full building floors where slab panels were continuous over their boundaries.

The objective of this research is to assess the SPM capabilities by comparing with VULCAN models. As SPM is based on isolated slab panel, to be comparative with SPM, a VULCAN model that validates its capability for modelling an isolated slab panel is important.

BRE Garston test (Bailey, 2000) has been introduced in Section 2.3.2. It was an ambient temperature test that was designed particularly for simulating an isolated slab panel behaviour in fire.

In a real fire, the loads above the floor stay unchanged, but the load – carrying capacity of the structural members decreases in elevated temperature until failure. On the other hand, Garston ambient temperature test used a simply supported slab without any load – carrying capacity by increasing load to simulate floor structural response in elevated temperatures.

In the Garston ambient temperature test, the slab panel was initially designed to reach its maximum load – carrying capacity by its self-loading. During the test, the slab showed ambient temperature structural failure as soon as the steel deck was removed. This was to simulate building floor losing strength till it start exceeding its yield-line load carrying capacity in elevated temperature. As the loading above the slab increased, the slab deflected till integrity failure. This was to simulate floor's decreasing strength in elevated temperature. Therefore, the BRE Garston ambient temperature test adequately simulated slabs in fire and is suitable for VULCAN to model for validation purpose.

Modelling Garston test is different from the elevated temperature modelling in VULCAN. Normally, VULCAN models structure in fire by inputting the temperature profile into all the corresponding structural segments at each time step, as a result the output is structural response against time. However, as Garston test was in ambient condition, there was no temperature change but growing Uniform Distributed Load (UDL). Therefore, to be comparative to the test results, the temperatures for all structural elements are set to 20°C. The UDL value was set to 4.81 kN/m², which was the load at which the slab experienced integrity failure

(Bailey, 2000). The load increment in VULCAN is set to 1000 in order to apply UDL gradually on the slab.

In addition, as mentioned in Chapter 2, the grid size plays a significant role in VULCAN for accuracy and runtime. 1.5 m x 1.5 m and 1 m x 1m grid sizes have been used to model Garston test, but the models were interrupted due to calculation convergence. This is because the loads applied exceeded far beyond the slab panel's load – carrying capacity. These failed models showed VULCAN's limit, which is unable to model large areas of cracks. This is due to the fact that VULCAN uses smeared crack model, which assumes cracks spread within a whole grid surface once any crack occurs. For example, if a VULCAN modelled slab panel uses 1.5 m × 1.5 m grid size, VULCAN assumes an entire grid fails once any crack occurs on that grid.

To refine the model and obtain reasonable results, the model was re-ran with 0.5 m x 0.5 m grid size. Finally it was found that VULCAN was able to finish the modelling, however still experienced convergence. Figure 3-11 shows the comparison between the VULCAN model and the test data as mid span deflection against UDL.

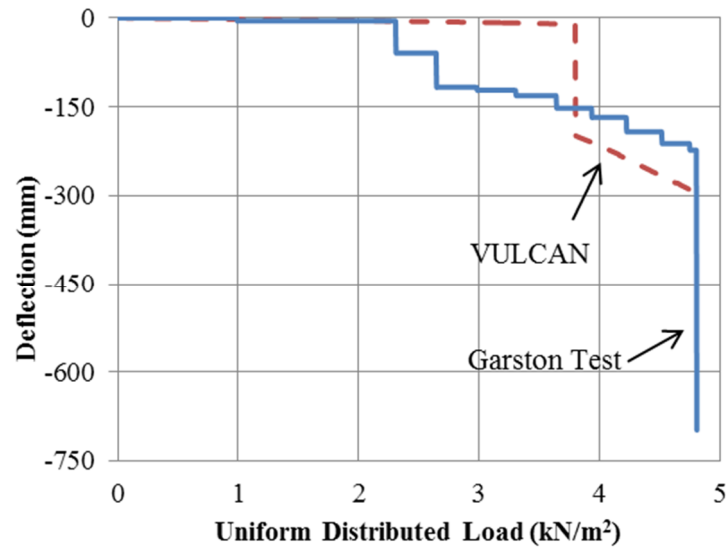


Figure 3-11: Comparison between VULCAN model and Gaston test data

It shows that VULCAN gives good agreement with the test data until UDL reached 2.3 kN/m². When the load reaches to 2.3 kN/m², the slab deflection increased rapidly whereas VULCAN gives no significant deflection. At approximately 3.8 kN/m², VULCAN deflection suddenly drops and becomes larger than the test data. Finally at 4.81 kN/m², the slab deflection drops down straight to 700 mm while VULCAN is only lowered to 300 mm.

The output showed that VULCAN was able to model the structural behaviour adequately before the concrete slab experience severe failure and predict the deflection with good accuracy for a period of time when the slab is undertaking load that is much larger than its capacity.

In reality the slab started cracking and deflection increased rapidly due to the extreme load applied to a concrete slab that had no load – carrying strength, it pushed VULCAN model to its limit as VULCAN was unable to calculate the structural response and showed convergence that presented as that straight line on the graph. However, in this research, the isolated slab panel is designed in conventional ambient temperature structural design so it is much stronger than

that in the BRE Gaston test. Therefore, VULCAN is suitable for modelling isolated slab panel in fire in this research. The grid size 1 m x 1 m was adopted in this research be due to time limitation. It is expected to predict the deflection with good accuracy.

3.3.2.2 Validation – Edge Beam Fire Protection Conditions in a Slab Panel

The deflection of the edge beams is dependent on the size and the fire protection applied to the edge beams. In the SPM design procedure, the edge beams deflection is provided by the SPM equations and results in a fixed value and it is based on the assumption of the edge beams are oversized or well protected. In VULCAN, the FEA analysis is able to simulate the deflection of the edge beams in fire. In this research, comparisons between the SPM and VULCAN were undertaken. As the edge beam sizes were designed to NZS3404 and fixed, the capability of VULCAN modelling the edge beam under various fire protection condition needs to be validated.

A 9 m x 9 m simply supported slab panel is initially investigated by modelling in VULCAN. As described in Section 3.1, in accordance with traditional ambient design, 460UB82.1 and 310UB40.4 were adopted as primary and secondary beams, respectively. A generic fire protection scheme was applied on the designed slab panel. The temperatures of the protected primary and edge secondary beams were limited to 550°C at 60 minutes of standard fire exposure. To achieve this, fire resisting gypsum boards (density = 800 kg/m³, specific heat capacity = 1700 J/kg/K, conductivity = 0.2W/mK) were used. Figure 3-12 shows the modelled slab panel.

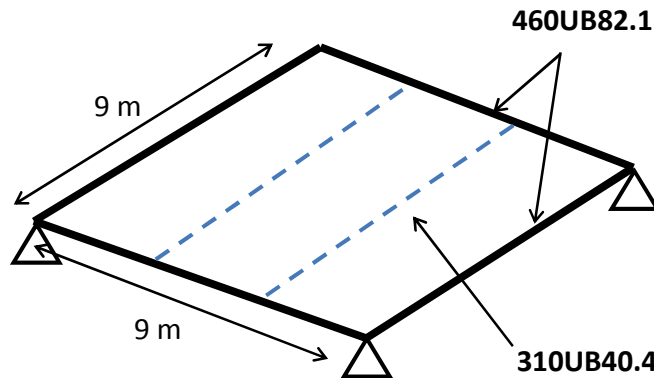


Figure 3-12: 9 m × 9 m modelled in VULCAN

Table 3-5 summarises several edge beam scenarios that were modelled in VULCAN. The initial VULCAN model V1 is a simply supported slab panel with a generic fire protection method having 550°C which has been described in Chapter 3. It is horizontally unrestrained with only vertical supports at the corners. The perimeter edge beams were protected and interior beams were unprotected. Other scenarios of perimeter edge beams contain edge beams with constant vertical supports (V2) which is consistent with the assumption of the Bailey method, overprotected edge beams (V3), “cold” edge beams (V4) that stay in ambient temperature.

Table 3-5: Vulcan analysis and Parameters

Support Conditions	VULCAN Analysis			
	V1	V2	V3	V4
Generic Protection	✓	✓		
2X Generic Protection			✓	
Cold Perimeter Beams				✓
Corner Vertical Restraint	✓	✓	✓	✓
Edge Vertical Restraint		✓		

The temperature curves of the each scenario have been calculated in a spreadsheet, in accordance with EC2 steel beam protected beam temperature equation (CEN, 2005). The temperature data of each scenario was then input into VULCAN.

The deflection curves obtained from VULCAN were compared with SPM limit deflection and maximum deflection. Limiting deflection is the deflection required to produce the enhanced load carrying capacity. Maximum deflection is the limiting deflection plus an edge-beam deflection which is span/100, in accordance with Clifton (2006). Figure 3-13 shows the SPM limiting deflection and maximum deflection of the 9 m x 9 m slab panel.

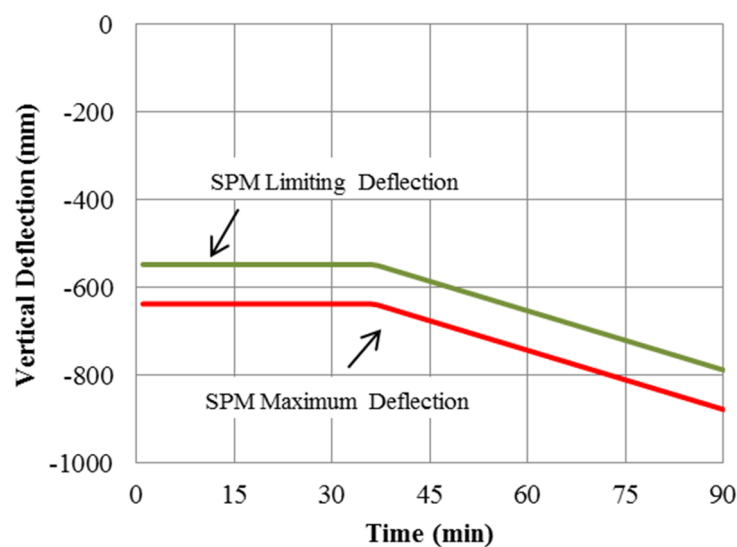


Figure 3-13: SPM Limiting Deflection and maximum Deflection

VULCAN central deflections and edge beam deflections were compared with SPM's limiting and maximum deflections. VULCAN provides the deflection-time history throughout the fire, whereas SPM predicts the deflection at the time of the fire resistance rating. Therefore, for the designed 60 minutes fire resistance rating slab panel, comparisons between SPM and VULCAN only occur at 60 minutes.

Since the results from VULCAN were compared with the SPM predicted deflection, Uniform Distributed Load (UDL) applied to the VULCAN model needs to be comparative to the SPM. SPM uses slab panel's limiting deflection as input to calculate the tensile membrane enhanced load – carrying capacity. This means that designed slab panel is expected to experience the limiting deflection when it is under the load that is equal to the predicted capacity. Therefore, the SPM predicted load – carrying capacity value W_u was used as the UDL value to apply to the VULCAN model.

Figure 3-14 shows the deflections of an isolated slab panel V1 obtained from VULCAN. Since the interior secondary beams were unprotected, they lost considerable bending capacity quickly so that the slab panel can deform largely in two-way in the centre and transfer load to the edge beams to form tensile membrane action. The deflection curve indicates that under elevated temperature the slab panel centre deforms fast until 15 minutes when the deformation slows down. This is due to the increased load – carrying capacity, as a result of the occurrence of tensile membrane action. However the results indicates that after 45 minutes the slab panel central deflection start failing, associated with accelerating deflection at the edge secondary and primary beams. As shown in the figure, the secondary beam deflects largely and approaches the central deflection. This indicates the formation of premature single-curvature mechanism failure due to weak edge secondary beams.

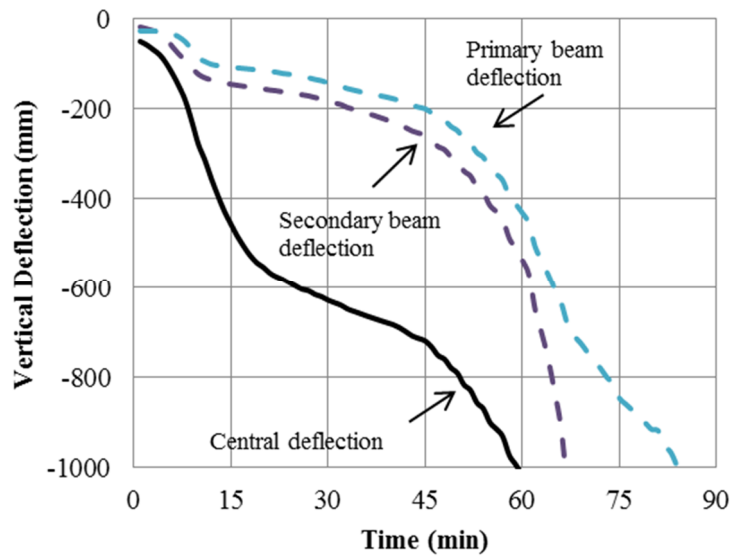


Figure 3-14: Central and edge beam deflections of 9 m × 9 m isolated slab panel

Figure 3-15 shows the SPM and VULCAN deflections together. In terms of VUCLAN results, it gives another way of demonstrating the slab panel deformations. It shows the relative central deflection of the protected primary and secondary beams. The relative deflection is the difference between the central deflection and the edge beam deflection. This demonstration is appropriate because the SPM predicted deflection uses a limited deflection on edge beams, which is also the difference between the central deflection and edge beam deflection. Similar demonstrations of the comparison between the Bailey method and VULCAN have been done by Abu *et al* (2012). Thus, to be comparative to the SPM, relative edge beam deflection was extracted from VULCAN results.

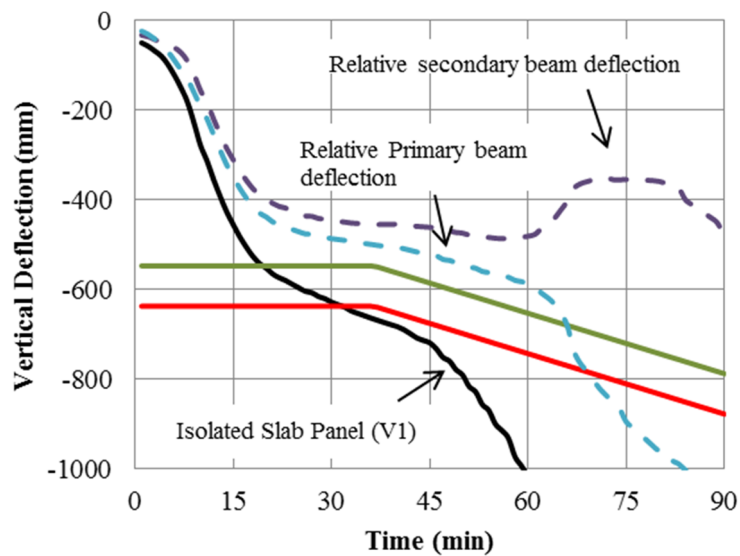


Figure 3-15: Isolated slab panel midspan and edge beam relative deflections (Gu *et al*, 2013)

As shown in Figure 3-15, deflection of the slab centre relative to the protected primary beams has a steady difference from central deflection which means that the primary beam deflects by following the central deflection. On the other hand, the relative secondary beam deflection shows similar trend as the relative primary beams but starts reducing after 60 minutes. This means that the difference between the central deflection and the secondary beam deflection decreases. It is consistent with Figure 3-14, which indicates that secondary beam bend closer to the central deflection, starts failing and produces extremely large deformation, and forms a single – curvature mechanism. It indicates that the strength of edge beams in a slab panel is significant for the tensile membrane action enhancing the slab panel.

In addition to the comparison between VULCAN central and relative edge beam deflections, comparison was undertaken between the VULCAN and SPM deflections. At 60 minutes, VULCAN shows the central deflection reaches 1000 mm while SPM predicts the maximum deflection is approximately 750 mm. However, the VULCAN relative deflections are less than

SPM's limiting deflection. This indicates that SPM predicted edge beam deflection is less than VUCLAN's edge beam deflection. Therefore, in this scenario the SPM's limiting and maximum deflections are not conservative by comparing with VULCAN's deflection. This is driven by the edge beam deflections which are taken by SPM as being span/75 or 120mm at the target FRR = 60 minutes. Figure 3-14 shows that the edge beam deflections from Vulcan are close to the SPM taken value of 120mm up to around 30 minutes, then increase slowly to 45 minutes then increase more rapidly, Figure 3-15 shows that the comparison of slab panel central deflection between Vulcan and SPM is close between 30 and 45 minutes and then diverges due to the rapidly increasing edge beam deflections. This illustrates the importance of the edge beams maintaining their effective strength and stiffness as edge supports in order for the SPM predictions to be accurate.

According to Figure 3-15, the protected edge secondary beam is more vulnerable than the protected edge primary beam. It shows that the whole slab panel fire resistance is driven by edge secondary beam's strength from 45 minutes of standard fire exposure onwards.

Therefore, for slab panels V2, V3 and V4, only their central deflections and relative secondary beam deflections are shown in the figures below, as they are more critical than primary beam deflections. These deflections are not only compared with V1 to present the significance of edge beam effect, they are also compared with SPM to assess the SPM's capability in predicting edge beam deflections.

Figure 3-16 shows the midspan deflections of V1 and V2, which is the slab panel with constant vertical support around the edges. It does not show the edge beam deflections of V2 because constant vertical support under the edge beams is assumed. In contrast, V1 suffered secondary

beam failure as shown in Figure 3-15, but V2 presents much lower deflection because of zero deflection at the edges. Therefore, this scenario confirms that the edge beams deflection has substantial contribution to the overall fire resistance of the whole panel.

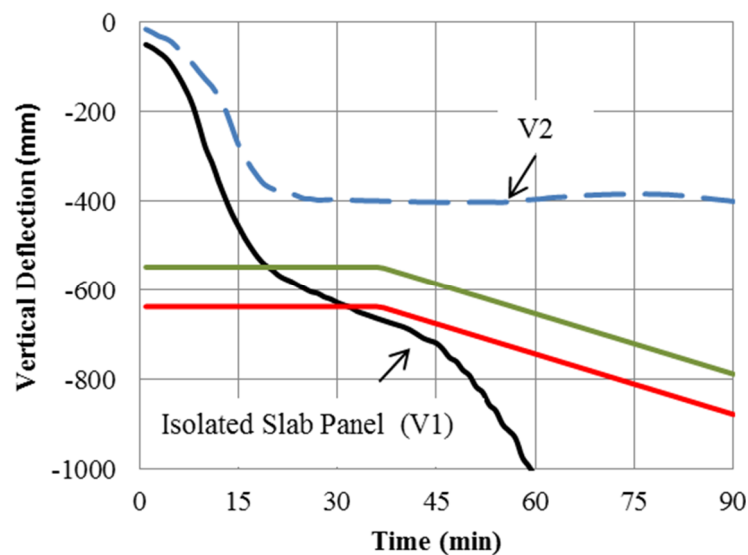


Figure 3-16: Comparison between midspan deflections of slab panel (V2) with corner vertical restraint and constant vertical support around the edges

Figure 3-17 shows the deflections of V3 which has overprotected ($2 \times$ generic protection thickness) edge beams. Because of this overprotection, the temperatures of V3's edge beams are much cooler than V1's. As a result, Figure 3-17 shows that V3's relative secondary deflection does not turn back as V1. Therefore, the overprotected edge secondary beam does not fail and the central deflection decreases slowly. The difference between V3's central deflection and relative secondary deflection remained constant after tensile membrane action occurred.

Comparing with SPM's deflections, V3's deflections are less than SPM's deflection at 60 minutes. It shows that V3 mid-span deflection at 60 minutes is close to the SPM's maximum deflection, but the relative secondary deflection is still less than SPM's limiting deflection. This

indicates that SPM predicts V3 scenario conservatively for the maximum central deflection of the slab panel, but it is not conservative on the edge beam deflection.

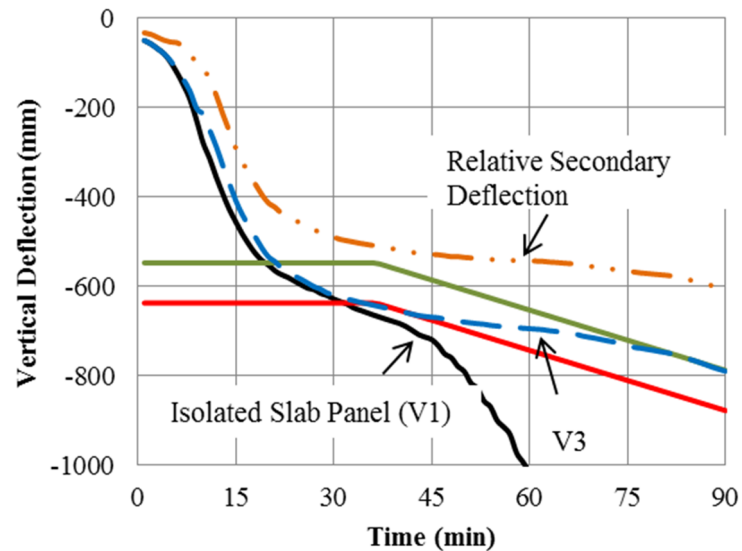


Figure 3-17: Comparison between deflections of isolated slab panel and slab panel (V3) with overprotected edges

Figure 3-18 shows the deflection of V4 which is the slab panel with cold edge beams. At 60 minutes, not only the midspan deflection gives good agreement with the SPM maximum deflection, the relative secondary beam deflection is almost as same as the SPM limiting deflection.

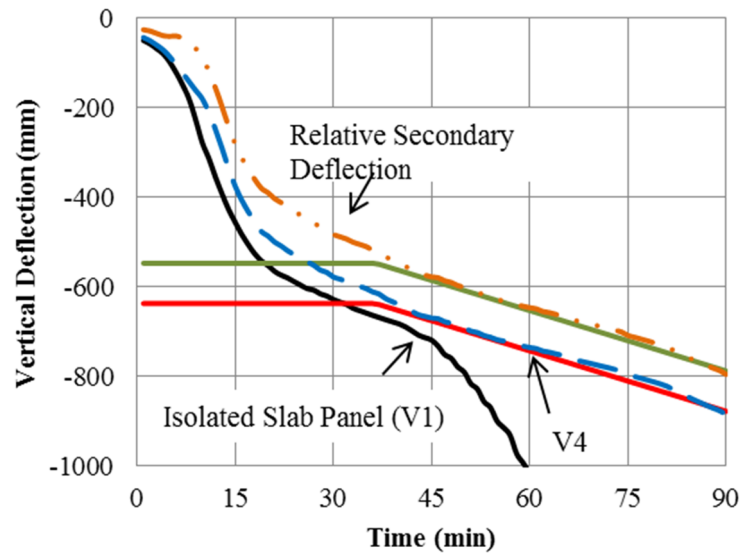


Figure 3-18: Comparison between deflections of isolated slab panel and slab pane with cold edges

Protected primary and secondary edge beams and deflections from V1, V3 and V4 were extracted from the results above and compared in Figure 3-19 and Figure 3-20, respectively. Both of them confirm that the edge beams deflections in fire are dependent on the fire protection, which determines the actual steel temperature. The normal generic protection (V1) causes approximately about 400 and 450 mm on the primary beams and secondary beams, respectively. After 60 minutes, the primary and secondary beams experiences severe deflections that lead to failure of the whole slab. On the other hand, doubling the thickness of protection (V3) and keeping the edge beams (V4) in ambient temperature cause much smaller deflection than V1. V3's protection keeps the edge beam deflections less than 200 mm, while V4's ambient temperature beam deflection is less than 100 mm.

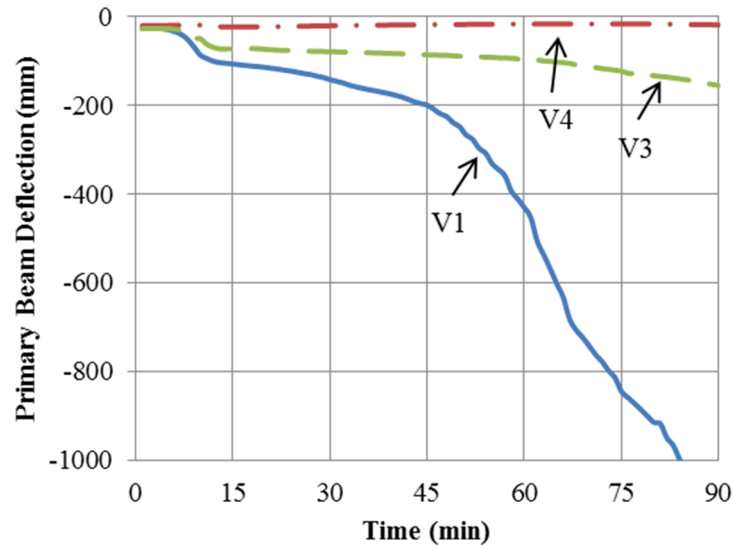


Figure 3-19: Comparisons between primary beam deflections

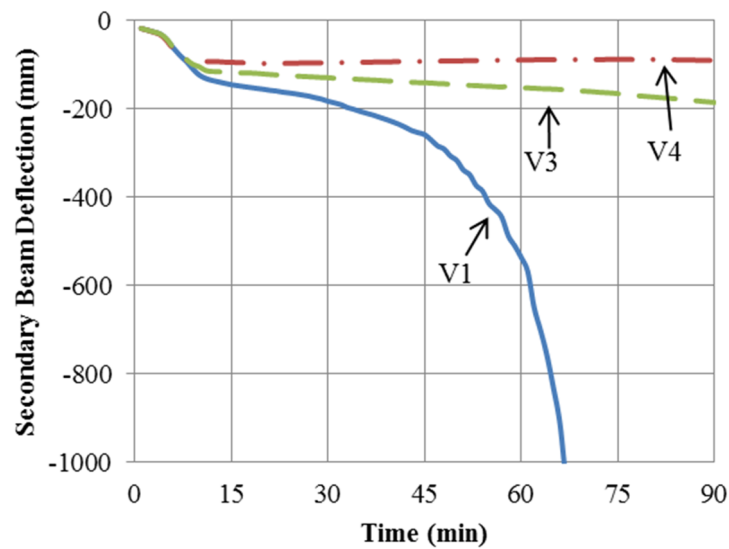


Figure 3-20: Comparisons between secondary beam deflections

According to the comparisons above, slab panel with various edge beam protection scenarios were modelled in VULCAN. Central and edge beams deflection were compared with each other, and also compared with SPM predicted deflection. The VULCAN models proved that the effect of edge beam deformation significantly influences the central deflection of a slab panel. The comparisons between VULCAN and SPM among those scenarios implies that the SPM is capable

to predict deflections of slab panel with strong or well – protected edge beams, consistent with the edge beam vertical deflection limit of span/75 built into the SPM procedure.

3.4 Comparisons

3.4.1 Edge Beam Stability under Various Slab Continuities

The objective of this research is to investigate the effectiveness of edge-beam support in the SPM where slab continuity is concerned. Therefore, the effect of various support conditions of the fire resistance of the slab panel is investigated by modelling in VULCAN.

It is important to note that full floor with multiple slab panels were not modelled, only one isolated slab panel was modelled. The variation of support conditions were simulated by changing the boundary condition of the slab panel.

Comparisons of VULCAN deflections were undertaken to assess the effect of different number of continuity to the fire resistance of each targeted slab panel. Those deflections were also compared with SPM predicted deflections to assess the capability of SPM in estimating the internal slab panel deflections.

Slab panels with different number of continuity S1 to S6 are shown on Figure 3-21. The solid and dashed lines refer to the edge and the unprotected secondary beams, respectively. S1 shows an isolated slab panel with four external edges, whereas Figure S2 to S5 shows different realistic slab panel possibilities, i.e. slab panels with different numbers of sides continuous. S2 is a slab panel with two adjacent internal edges, S3 and S5 are slab panels with three internal edges, and S4 is a slab panel with four internal edges.

There are two scenarios each for two sides and three sides continuous. Each of them would have a different behaviour, as slab continuity across primary and protected secondary beams would result in different slab panel behaviour. For slab continuity on two sides, the internal edges can be adjacent or opposite, so S6 shows a slab panel with two opposite internal edges. For three internal edges, two of the internal edges can across the protected secondary beams or primary beams as shown in S3 and S5.

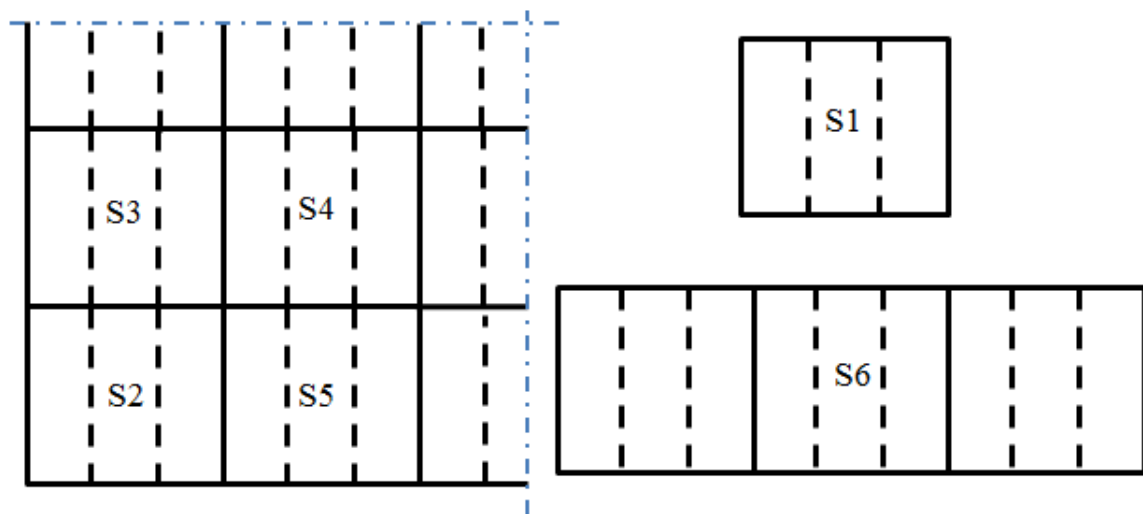


Figure 3-21: 9 m × 9 m slab panels with different number of continuity from S1 to S6 (Gu *et al*, 2013)

For all the VULCAN modelled slab panels in the various boundary conditions, the boundary conditions of each panel were altered from the simply supported slab panel (S1). At the continuous side, additional stiffness applies on the boundary, where the steel edge beam of the panel is rotational restrained by the continuous concrete slab running over it. Therefore the central deflection and their edge beam deflections were influenced by the number of continuous edges.

3.4.2 Aspect Ratio

Futhermore, the effect of aspect ratio was investigated in this research. Previous research (Bailey, 2003b) indicated that the aspect ratio, which is the ratio of the length of the longer side to the shorter side, could influence the effectiveness of tensile membrane action and the pattern of failure. In this research, apart from square slab panel (9 m × 9 m), another two slab panels 9 m × 6 m, 9 m × 12 m (Figure 3-22) were also investigated. The sizes of slab panels used are same as recent research (Abu *et al.*, 2012),

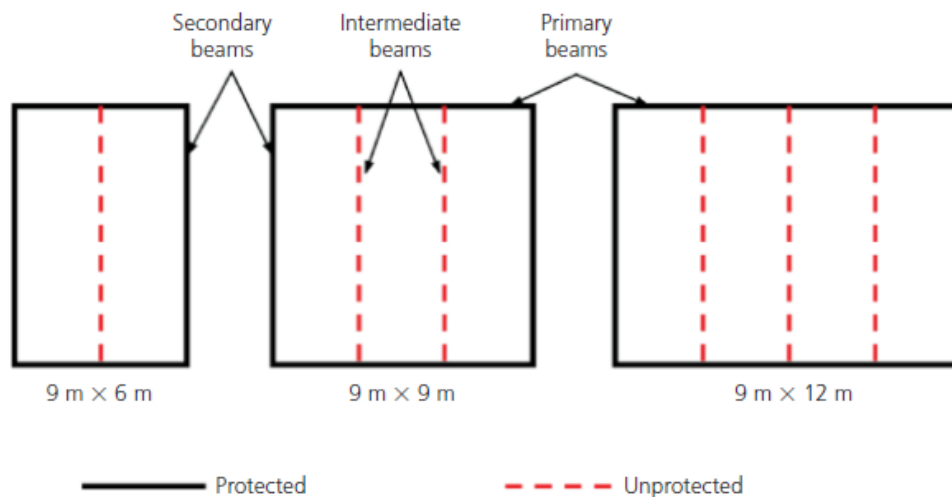


Figure 3-22: Three sizes slab panels are modelled in this research (Abu *et al.*, 2012)

Same as the procedure used on the 9 m × 9 m slab panel, the VULCAN modelled isolated slab panels 9 m × 6 m and 9 m × 12 m are loaded to their own ultimate capacity and compared with SPM limiting and maximum deflections. These slab panels were modelled and compared with various number of continuity from S1 to S6 and loaded under fire limit state load.

Conclusion

In conclusion, this chapter covers the methodology and preparation for the models, as follows:

- A 9 m x 9 m slab panel was initially modelled in this research.
- The composite beams of the slab panel were designed in ambient temperature and have a 60min Fire Resistance Rating (FRR).
- Thermal analysis and structural analysis were both conducted in the SPM and VULCAN, respectively.
- SPM uses equations to determine steel beam, reinforcement and slab temperatures, while VULCAN uses concrete and reinforcement temperature from ABAQUS, steel temperature from Eurocode 3 (CEN, 2005).
- A validation of VULCAN was undertaken by modelling the BRE-Gaston. The results showed:
 - VULCAN can predict the deflection with good accuracy when the slab is undertaking load that is much larger than its capacity before severe failure. Therefore it is suitable to use VULCAN to model isolated slab panel and compare with the SPM.
 - 1 m x 1m grid size is suitable for modelling slab panel's structural response in fire.
- A validation of the capability of VULCAN modelling slab panels with various edge beam fire protection conditions was undertaken. The VULCAN model scenarios showed that the SPM is capable to predict deflections of slab panel with well – protected edge beams.

After the thermal and structural analysis and validations, the SPM and VULCAN model can be compared with each other. As mentioned in Section 3.4, comparisons of VULCAN and the SPM models were undertaken to check the effect of various continuities on the edge beams and the capability of the SPM.

4 COMPARISONS OF VULCAN AND THE SPM MODELS

Introduction

Chapter 3 described the modelling of the 9 m x 9 m slab panel in VULCAN and the SPM. It explained why certain design and modelling options were made. This chapter provides the results and analysis of the models and comparisons between VULCAN and the SPM models.

4.1 Edge Beam Stability under Various Continuities

As described in Section 3.4.1, six 9 m x 9 m slab panels S1 – S6, were modelled by VULCAN and compared with the SPM to investigate the effect of various boundary conditions on the slab panel's edge beam stability. Slab panels' central deflection and their edge beam deflection were shown, and they were compared with the SPM limiting and maximum deflection.

Figure 3-15 shows the V1 (S1) central deflection and its relative primary and secondary deflections. As explained in section 3.3.2.2, the decreasing relative secondary beam deflection after 60 minutes indicates the edge secondary beam starts failing and the central deflection starts increasing rapidly due to the failure of the secondary beam. It also indicates that SPM's assumption for isolated slab panel edge beam of span/75 is not stability are not conservative for those particular edge beams.

S2 is a slab panel that has two adjacent internal edges. Figure 4-1 shows the deflections at the centre and at the midpoint of the external beams. At 60 minutes the external primary beam and external secondary beam reach 100 mm and 200 mm, respectively. After 60 minutes, the

rate of their deflection increases and their deflections are finally close to central deflection at 90 minutes.

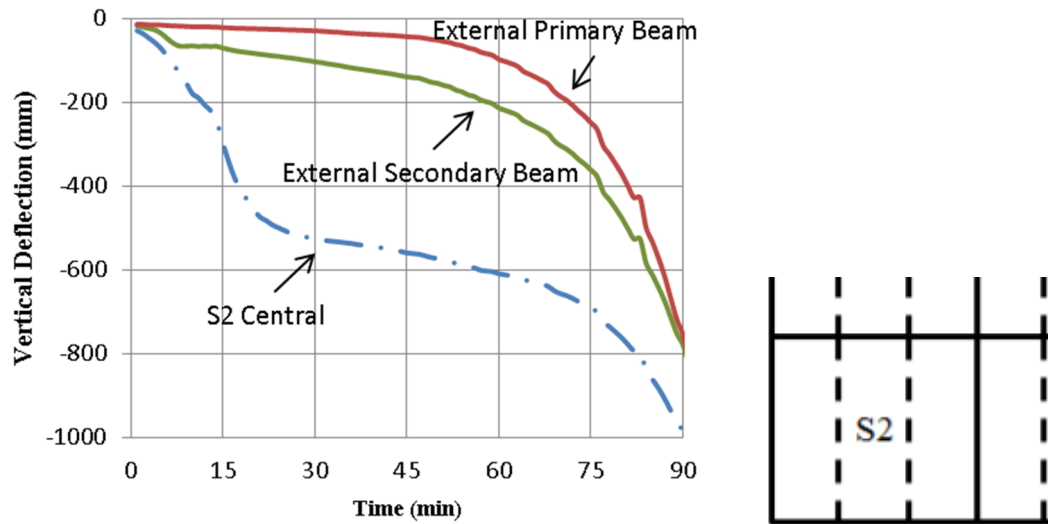


Figure 4-1: S2 central and non-continuous primary and secondary beam deflection

Figure 4-2 shows the deflections of the internal edge beams. The results show that the internal edges experienced slight deflections which are less than 1.0 mm. At 60 minutes the vertical deflection of the internal secondary beam and continuous primary beam reached approximately 0.58 mm. During the modelling, it was found that the internal edge beams had very minor deflections that are less than 1.0 mm. This is caused by the enhanced stiffness at the continuous boundaries. Therefore, the continuous edge beam deflections of other slab panels will not be presented as they have little contribution to the central deflections.

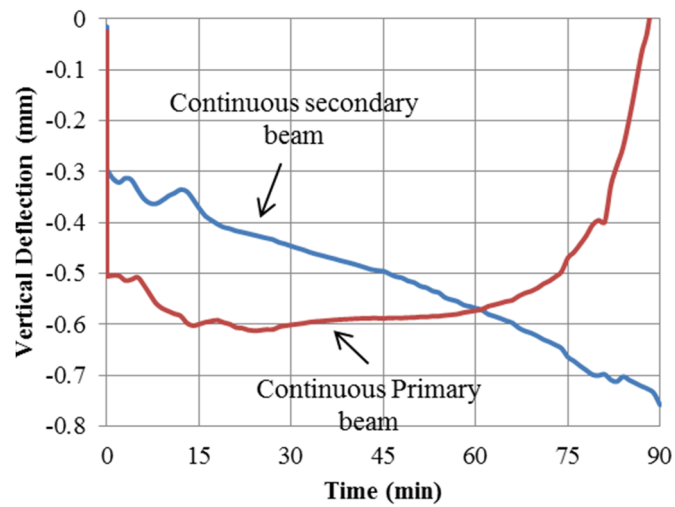


Figure 4-2: S2 continuous secondary and primary beams deflection

Slab panel S3 has two internal sides with primary beams and one internal side with a secondary beam, as shown in Figure 3-21 . Figure 4-3 shows the S3 central deflection and the deflection at its free edge. The central deflection curve of this slab is similar as S2 before 60 minutes. However, after 60 minutes, it deforms downwards at a slower rate as compared with S2. This is because S3 has one more continuous side than S2, which provides more stiffness to the entire slab panel. The external secondary beam of S3 reaches 200 mm deflection at the same time as S2 at 60 minutes. This also indicates that the extra edge with reinforcement continuing provides additional stiffness on the slab panel.

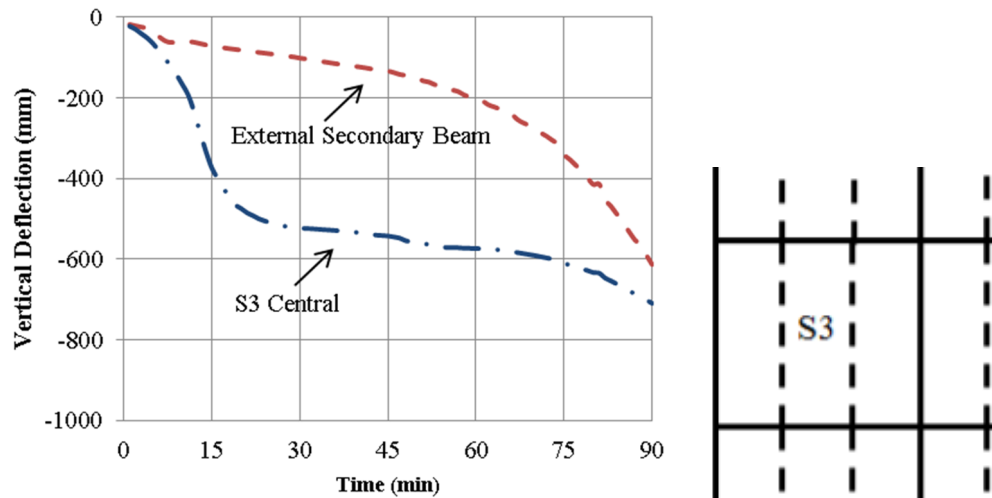


Figure 4-3: S3 central and non-continuous primary beam deflection

Another slab panel with three sides continuous is S5. As shown in Figure 3-21, S5 is different from S3 in terms of the number of the type of beams that are internal or external. It has two internal sides with secondary edge beams and one internal side with one primary edge beam. Figure 4-4 shows the S5 central deflection and the deflection at the edge primary beam. The central deflection curve of S5 is similar to those of S2 and S3. The external edge primary beam deflects to approximately 90 mm at 60 minutes and drops more quickly after that.

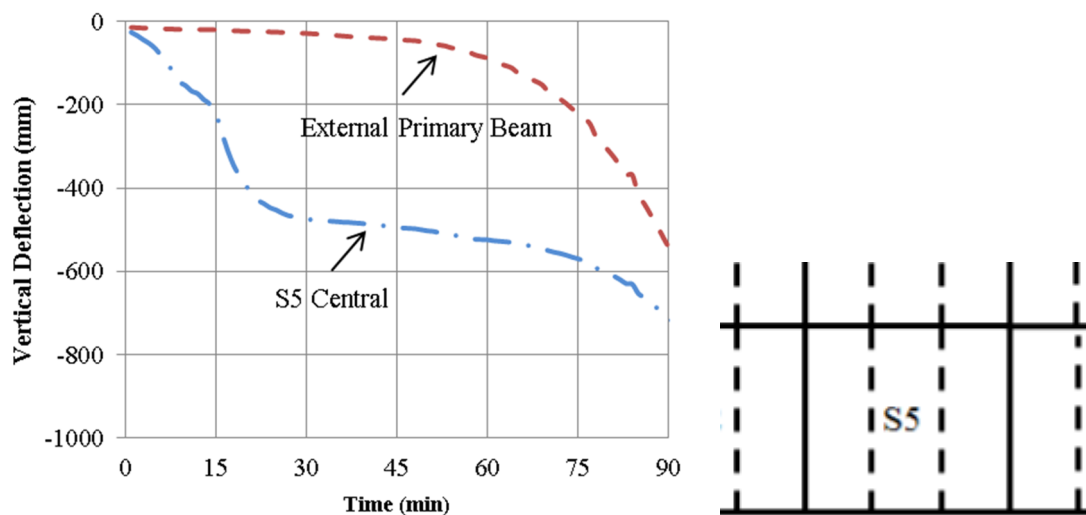


Figure 4-4: S5 central and non-continuous primary beam deflections

According to above, S2, S3 and S5 have similar deflection curves. Although their external beams drop down quickly after approximately 45 minutes, the central deflections of these slab panels do not follow the failing external edges, because the internal edges provide the slab panel more stability on their edges.

Since the S3 and S5 are similar slab panels but has different internal sides, Figure 4-5 shows the comparison between the S3 and S5. At 60 minutes, S3's external secondary beam reaches 200 mm while S5's external primary beam is at approximately 100mm. This indicates the primary beam is stronger than the secondary beam because the edge beam only starts to deflect after sufficient capacity has been lost internally.

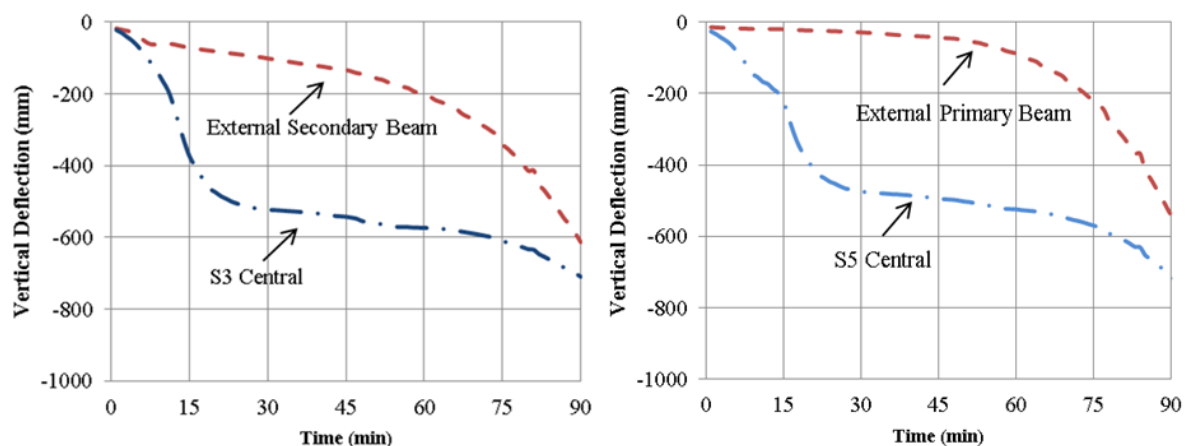


Figure 4-5: Comparison between S3 and S5 deflections

Figure 4-6 shows the central deflection of S4, which has all four internal edges. It only shows the central deflection, because its edge beam deflections are very small. The deflection curve shows that the S4 slab panel centre deflects down in the first 30 minutes, but the deformation becomes steady at approximately 490 mm and afterwards.

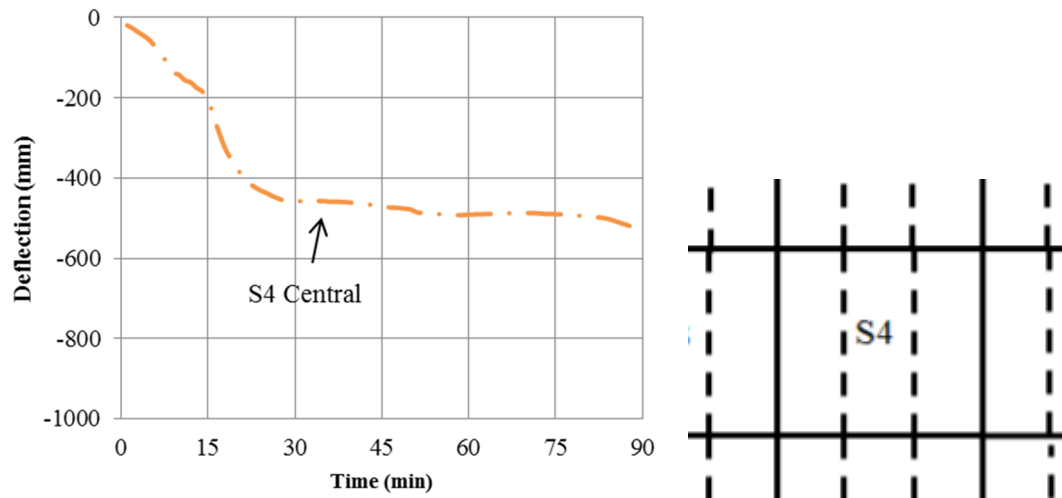


Figure 4-6: S4 central deflection

S6 is another slab panel with two continuous sides. However S6 has two continuous sides located at two opposite edge secondary beams. Figure 4-7 shows that S6 central deflection reaches approximately 790 mm at 60 minutes. Its external primary beam deflection starts to drop down until failure occurs after 45 minutes. It shows that the central deflection of S6 is driven by the two opposite external edge primary beams deflection. This is because extra stiffness are provided to the internal secondary beams and all the loads are transferred to the external edge beams.

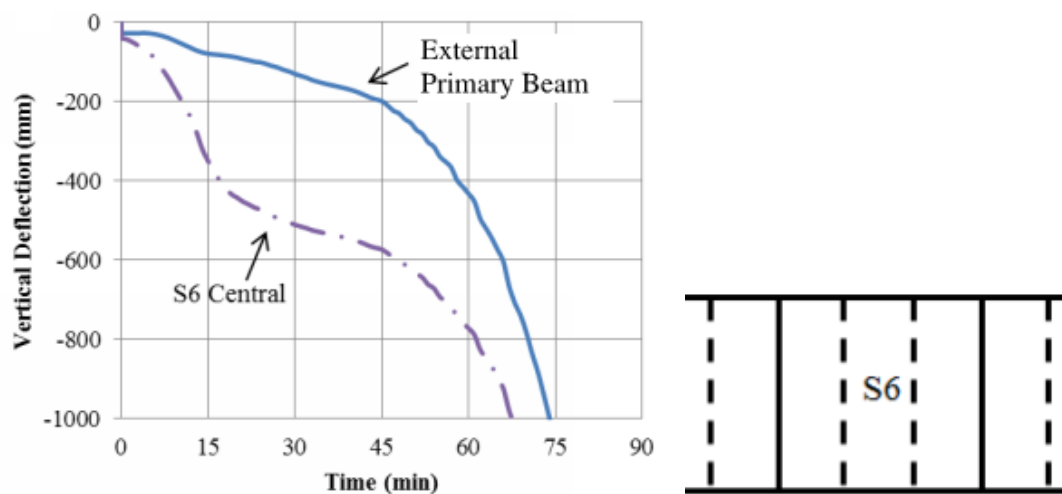


Figure 4-7: S6 central and non-continuous primary beam deflection

Overall, slab panels S1 – S6 with various numbers of internal edges have been modelled in VULCAN. Central and internal edge beam deflections were compared. The comparisons confirm that the internal edges positively contribute to the overall fire resistance of the slab panel.

In order to investigate the effect of the various continuities and compare with the SPM's limiting and maximum deflection, Figure 4-8 and Figure 4-9 below combine the S1 – S6 central deflections with SPM limiting and maximum deflections.

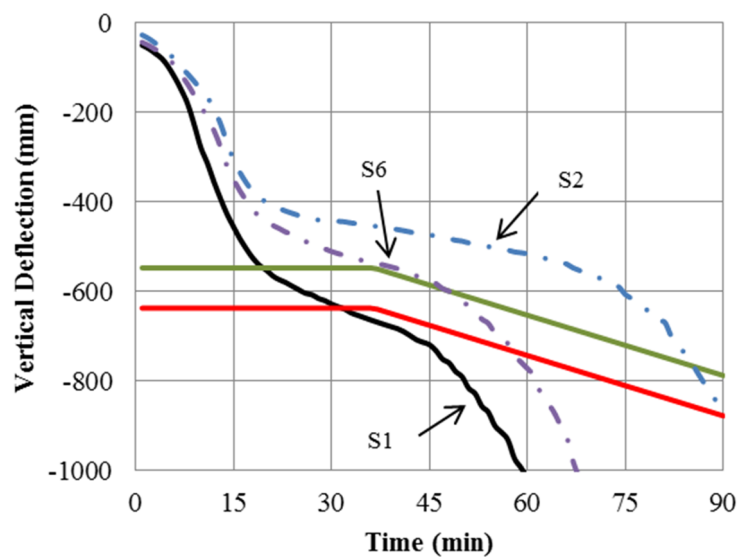


Figure 4-8: Central vertical deflection of a slab panel with two continuous sides (Gu *et al*, 2013)

As shown in Figure 4-8, S2 and S6 were plotted within the same figure as they both have two continuous sides. It clearly shows that an increase in the number of continuous edges results in a substantial increase in stiffness of the slab, by comparison with S1, which is a simply supported slab panel having zero continuous sides. It is observed that SPM overestimates the central deflections of panels which have continuous edges, while it under predicts the deflection of isolated slab panels. This is to be expected as the model is based on isolated

panels. Figure 4-8 also shows that a panel with two adjacent continuous sides performs better than that with continuity on two opposite sides. This is because S2 has an internal primary beam which is stronger than S6's internal secondary beam.

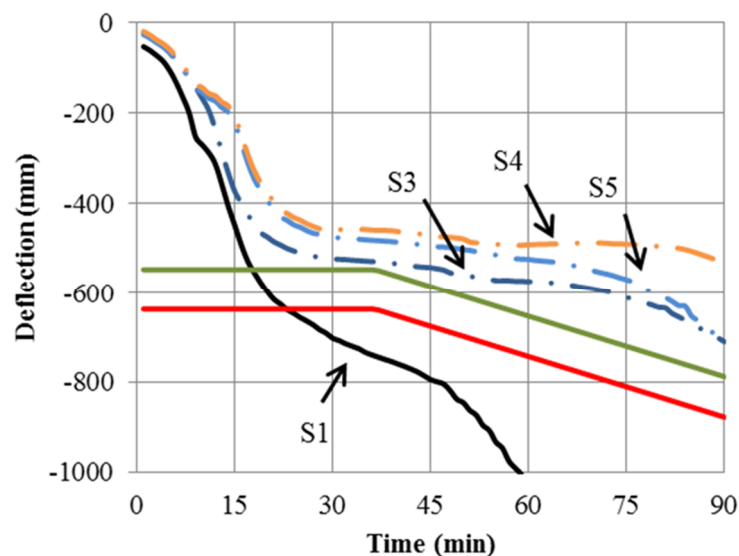


Figure 4-9: Central vertical deflections of the slab panel with various continuities (Gu *et al*, 2013)

Figure 4-9 contains the curves of S3, S4 and S5 and they are compared with S1 and the SPM deflections. At 60 minutes, S4 deflection is smaller than all other slab panels. This is expected as it has all four sides continuous. S3 deflects more than S5, although they have the same number of continuous sides. It indicates that the effect of edge secondary beams is more critical than the effect of edge primary beams within the designed slab panel.

According to the six slab panel scenarios above, the results indicate that continuity over the protected edge beams was beneficial to the stiffness of the slab panel. The SPM underestimated isolated slab panel deflections, because it underestimated the deflection of the edge beams, but provided conservative predictions of internal slab panel behaviour because it does not allow for the beneficial effect of tensile membrane stiffening over an internal support.

Without enough continuity and stiffness, the isolated slab panel exceeded 1000 mm deflection and was under pre-failure stage, where deflection increases nonlinearly with increasing rate of deflection.

The results above show that the design of the protected edge beams for the loadings from the yieldline area only are not sufficient to meet the SPM assumed edge beam deflection limit of span/75. This means that edge beams so designed could lead to premature edge beam failure and collapse of the whole slab panel. Therefore, the edge beam must be re-designed in order to meet the required fire resistance rating.

4.2 Re-Designed Edge Beam Stability under Various Continuities

It was expected that the VULCAN central deflection would meet the SPM limiting deflection under the SPM's capacity loading W_u , because in the SPM calculation, the load carrying capacity W_u is calculated according to the limiting deflection.

However, slab panel S1's central deflection and its relative secondary beam deflection showed the edge beam failed under the SPM's capacity loading. This indicates that the edge beam must be re-designed using the SPM capacity loading as design load.

W_u is transformed to distributed load by using the yield line pattern tributary area and is then applied to the edge beams. Figure 4-10 shows the yield line tributary area from which the supporting edge beams support the distributed load. The tributary areas for secondary beams are the triangle areas labelled as B and D with a height equals to L_1 . The tributary areas for primary beams are the trapezoid areas A and C. This feature has been included into the SPM design procedure (Clifton, 2006).

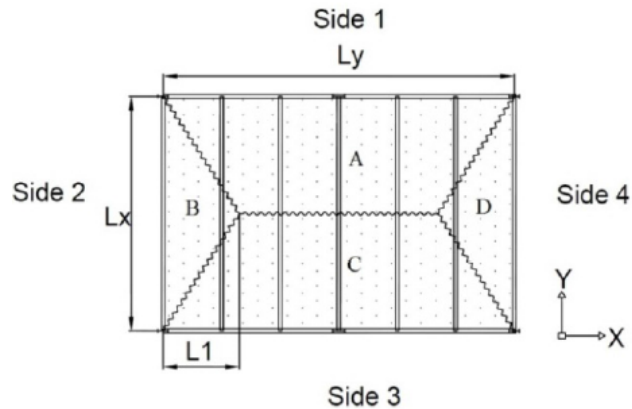


Figure 4-10: SPM yield-line pattern used in edge beam design (Clifton, 2002)

By following the SPM's design procedure, the protected primary and secondary beams were redesigned. The new slab panel is shown in Figure 4-11. 700WB130 and 460UB74.6 were adopted as primary and secondary edge beams. The interior secondary beams were kept as 310UB40.4. The new re-designed isolated slab panel is shown Figure 4-11.

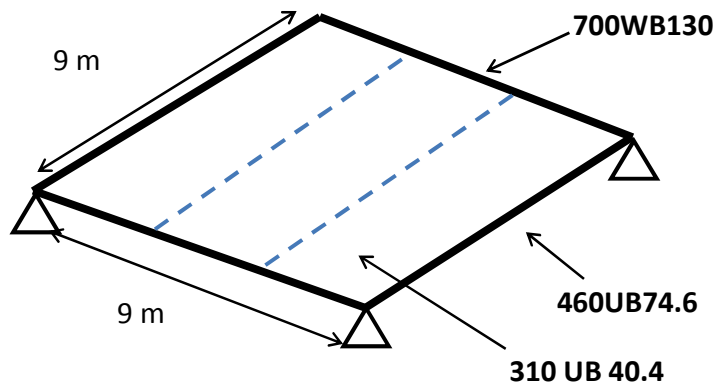


Figure 4-11: Redesigned 9 m x 9 m slab panel

The re-designed slab panel was modelled in VULCAN and compared with the SPM deflections again as shown in Figure 4-12. Figure 4-12 clearly demonstrates that the re-designed edge supporting beams provides significant enhancement to the overall fire resistance of the slab. At 60 minutes, VULCAN and the SPM predicted the central deflection to be 766 mm and 742 mm,

respectively. The comparison shows that the slab panel central deflections are similar around 20 minutes when the interior secondary beams lose strength but the re-designed slab panel deformed less due to the stronger edge beams.

The graph also indicates that the contribution from the secondary beam to the central deflection increases gradually as time progresses. The relative edge deflections indicate that the primary beam had little deflection while the secondary beam had an increasingly large deflection. Therefore, the comparisons indicate that edge beam stability is essential for using the SPM in structural fire design, given the span/75 edge beam deflection built into the procedure and the re-designed edge beams are suitable for the SPM isolated slab panel design.

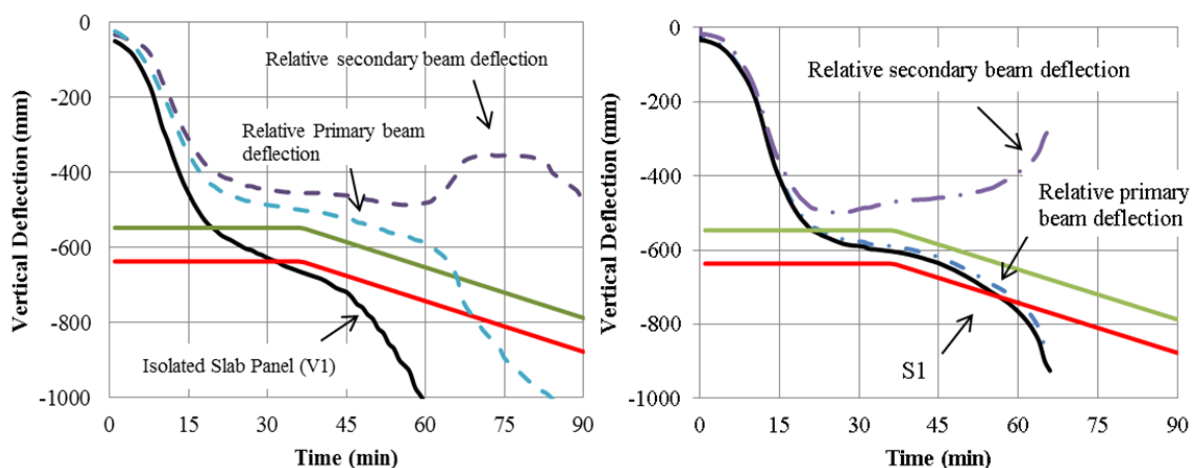


Figure 4-12: Comparison of original slab panel and re-designed slab panel

Similar to the original slab panels, the effect of various continuities on the stability of the slab panel was investigated. In the comparisons below, not only the re-designed slab panels deflection are shown, but also the original designed slab panel deflections are also attached, as shown in Figure 4-13 and Figure 4-14.

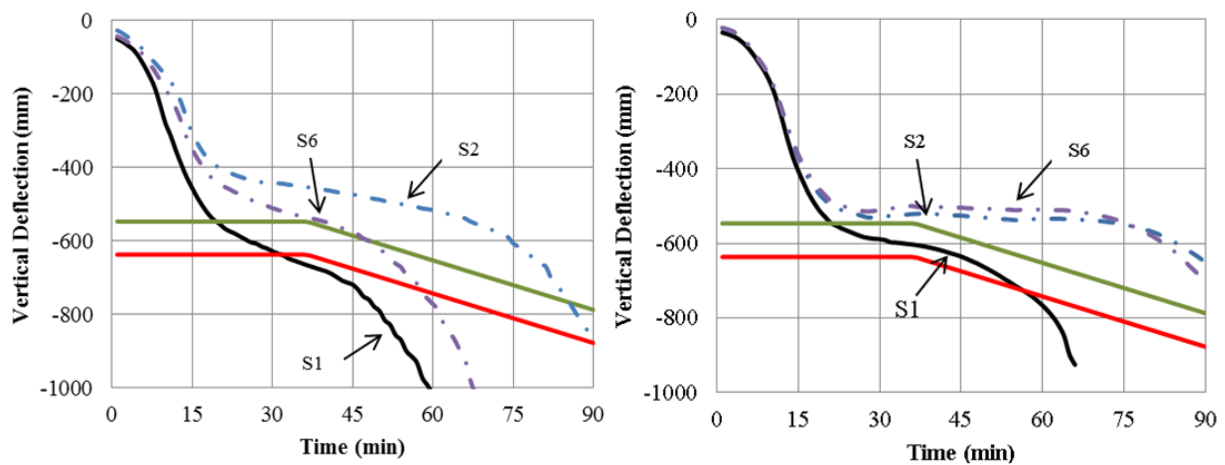


Figure 4-13: Central vertical deflection of a slab panel with two continuous sides. (Left: Original design slab panel. Right: Re-designed slab panel)

Figure 4-13 shows the deflection of S2 and S6 which compare with the isolated slab panel deflections and the SPM deflections. The deflection of S6 and S2 from the original slab panel shows an increase of difference and S6 exceeds the SPM maximum deflection at 60 minutes. The deflections from the re-designed slab panel shows S2 and S6 have similar deformation throughout the duration of fire. However, the S6 still has lower deflection than S2.

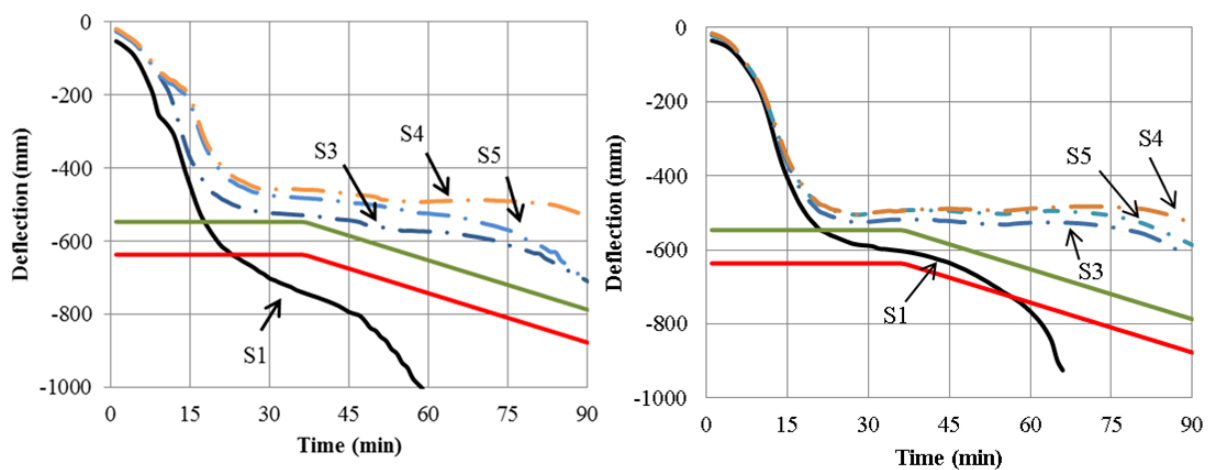


Figure 4-14: Central vertical deflection of a slab panel with various continuities. (Left: Original designed slab panel. Right: Re-designed slab panel)

Figure 4-14 shows S3, S4 and S5 deflections which compare with the isolated slab panel deflection and the SPM deflection limit. Similar to the original slab panel, S3, S4 and S5 slab panels have more stiffness provided by the continuous edges, so the central deflections are less than the SPM limiting deflection. Comparing S3, S4 and S5 with the original design, there were marginal differences between the original designed slab panel and the re-designed slab panel.

In summary, the above demonstrates the comparisons of the deflections of the re-designed slab panel, and the comparisons between the original slab panel and the redesigned slab panel. The VULCAN models clearly show the re-designed edge beams provide more stiffness to the slab panels. According to the models above, the edge beams are critical to the stability of the slab panels and the slab continuities over edge beams which provide rotational restraint already made the entire slab panel stronger. Therefore the re-designed edge beams are more beneficial to the isolated slab panel than the other slab panels with various numbers of internal edges.

4.3 Comparisons of SPM Required Deflection and VULCAN

In the comparisons detailed in section 4.2 , the VULCAN modelled slab panels were loaded to their maximum capacity in order to compare with limiting and maximum deflections of the SPM. However, the limitation of this approach is that it could only assess the SPM's capability in predicting isolated slab panel deflections because the limiting deflection and maximum deflection are not altered by the edge conditions.

To investigate the SPM's structural responses from the effect of various slab continuity conditions in fire, the SPM required deflections were calculated and compared with the VULCAN modelled slab panels under the fire limit state loads.

During standard fire exposure, the yield line capacity decreases as the composite slab and steel beams lose their strength. When the load carrying capacity decreases to a certain level below the design action, tensile membrane enhancement takes part in enhancing the yield line capacity. This is the core of the SPM design. Therefore, the required deflections of the SPM were derived by back calculating from the increase in capacity required for tensile membrane action.

The re-designed SPM edge beams were used in this comparison. The panels were loaded with $G + 0.4Q$. Slab panels' required deflections S1 – S6 are shown in Figure 4-15. It illustrates that the deflections became smaller from S1 to S6.

This means that the required deflection for producing tensile membrane action enhancement decreases as a result of increases in yield line capacity with increasing number of continuous edges. VULCAN modelled S1 - S6 deflections subject to fire limit state load are also shown in Figure 4-15. To show that different loading scenario is applied in this comparison, the S1 slab panel under the SPM capacity load W_u is shown in the same graph.

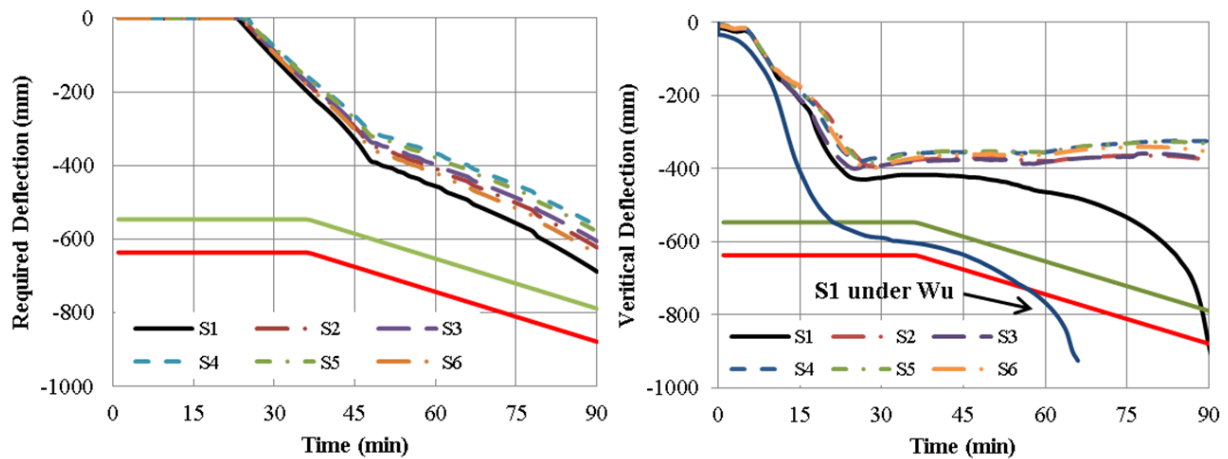


Figure 4-15: SPM – 9 m × 9 m slab panel, required deflections (Left) and VULCAN – 9 m × 9 m slab panel, central vertical deflections (Right).

In comparison, the deflections of the simply supported slab panel modelled by SPM and VULCAN S1 at 60 minutes are the same at approximately 460 mm. Within both the SPM and VULCAN models, the deflections showed similar behaviour of slab panels with their corresponding continuity: with increasing numbers of continuous edges, the deflections decrease. In comparison with the SPM required deflection and VULCAN deflection, SPM was conservative in predicting the effect of increasing number of continuous edges by comparing with deflections generated in VULCAN. In addition, the SPM required deflection did not exceed the SPM limiting deflection which means the slab panel did not collapse. However, the VULCAN deflections of the isolated slab panel indicated the slab panel experienced increasing rate of deflection from 75 minutes.

4.4 Effect of Aspect Ratio

Introduction

As mentioned in Section 3.4.2, the aspect ratio can influence the effectiveness of tensile membrane action and the pattern of failure. Therefore, apart from the 9 m x 9 m slab panel, 9 m x 6 m and 9 m x 12 m slab panels were investigated to check for the effect of aspect ratio on edge beam stability.

This section shows the SPM and VULCAN modelled 9 m x 6 m, 9 m x 12 m slab panels and the corresponding comparisons. Same as the procedure used for the 9 m x 9 m slab panel, the VULCAN modelled isolated slab panels 9 m x 6 m and 9 m x 12 m were loaded to their own ultimate capacity and compared with SPM limiting and maximum deflections. These slab panels were also modelled and compared with the SPM required deflections with various number of side continuity from S1 to S6 and loaded under fire limit state load.

4.4.1 Slab Panels Description

The properties of the concrete slab are the same as those mentioned in Chapter 3. Same as the 9 m x 9 m panel, all the slab panels were designed to 60 minutes fire resistance under 90 minutes standard fire exposure. The edge beam design was under each slab panel's corresponding W_u , the summary of the steel beam sizes is shown in Table 4-1.

Table 4-1: Edge beam design data for 60 minutes fire resistance rating

Slab panel size	SPM design load (kPa)	Beam type	Beam section	Load ratio	Limiting temperature (°C)	Temperature at 60minutes (°C)
9 m × 9 m	9.42	Secondary	460UB74.6	0.455	591	544
		Primary	700WB130	0.432	606	530
9 m × 12 m	6.49	Secondary	410UB59.7	0.462	586	546
		Primary	800WB146	0.419	615	534
9 m × 6 m	15.8	Secondary	530UB92.4	0.473	578	524
		Primary	610UB113	0.466	583	529

4.4.2 9m x 12m Slab Panel

4.4.2.1 9 m x 12 m Isolated slab panel

An isolated 9 m x 12 m slab panel was modelled first. Figure 4-16 compares its SPM limiting and maximum deflections with VULCAN modelled slab panel under its SPM capacity loading. It shows the central deflection at 60 minutes is very close to the SPM limiting deflection. This indicates that the SPM designed slab panel provides good estimation of the whole 9 m × 12 m slab fire resistance. However, the relative secondary beam deflection start decreasing at 60 minutes which means the edge secondary beam starts failing. As shown in the figure, the slab panel fails rapidly after 60 minutes. Therefore, the SPM edge beam deflection limit underestimates the edge beam deflection.

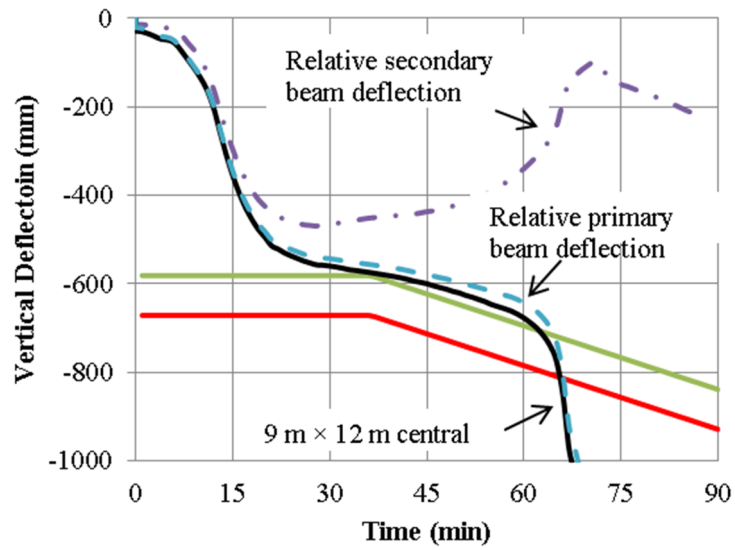


Figure 4-16: 9 m \times 12 m comparison between VULCAN and SPM central deflection

4.4.2.2 9 m \times 12 m Slab Panel with Various Continuities

9 m \times 12 m slab panels with various numbers of continuities were modelled, as shown in Figure 4-17.

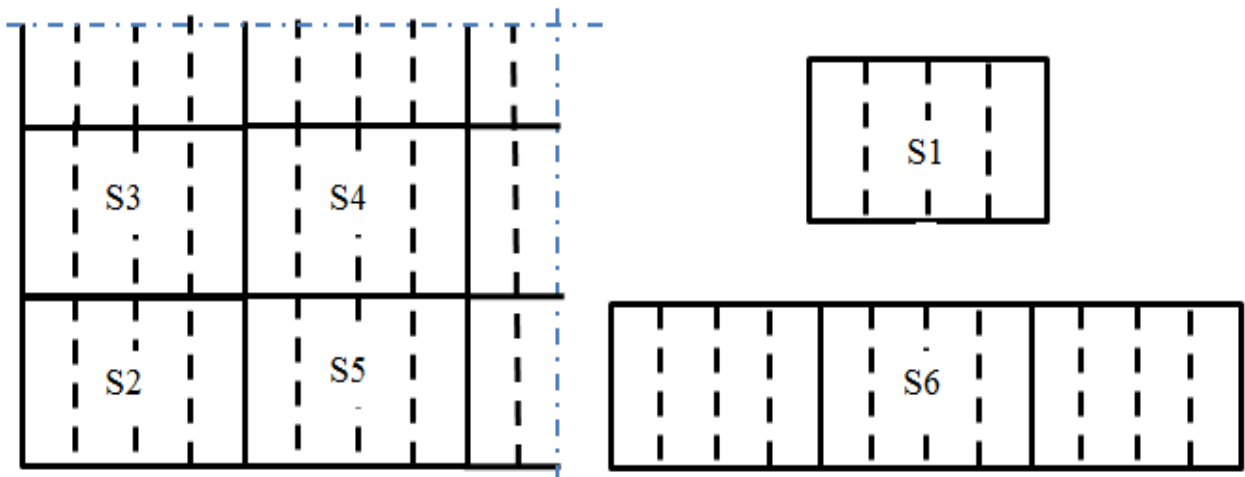


Figure 4-17: 9 m \times 12 m slab panels with different number of internal edges from S1 to S6

Figure 4-18 shows the required vertical deflections for SPM and the predicted actual deflections from VULCAN of slab panels S1 to S6. The deflections demonstrate that more stiffness was provided via the continuous edges and they provide more stability to the whole slab panel.

These results showed similar behaviour of the slab panels with various numbers of continuous edges as the 9 m x 9 m slab panel models. The SPM required deflection of the isolated slab panel reached approximately 700 mm at 60 minutes, and also exceeded the SPM maximum deflection at 70 minutes. It implies that the slab panel collapsed at 70 minutes. Same as other 9 m x 12 m slab panels with continuous edges, they followed the same trend as the isolated slab panel and failed later.

The VULCAN analysis shows 500mm deflection at 60 minutes which is much less than the SPM required deflection. However, VULCAN model started collapsing around 75 minutes which is close to the SPM required deflection, but other slab panels with continuous edges were stronger and did not fail. This is due to the extra stiffness provided from the edges.

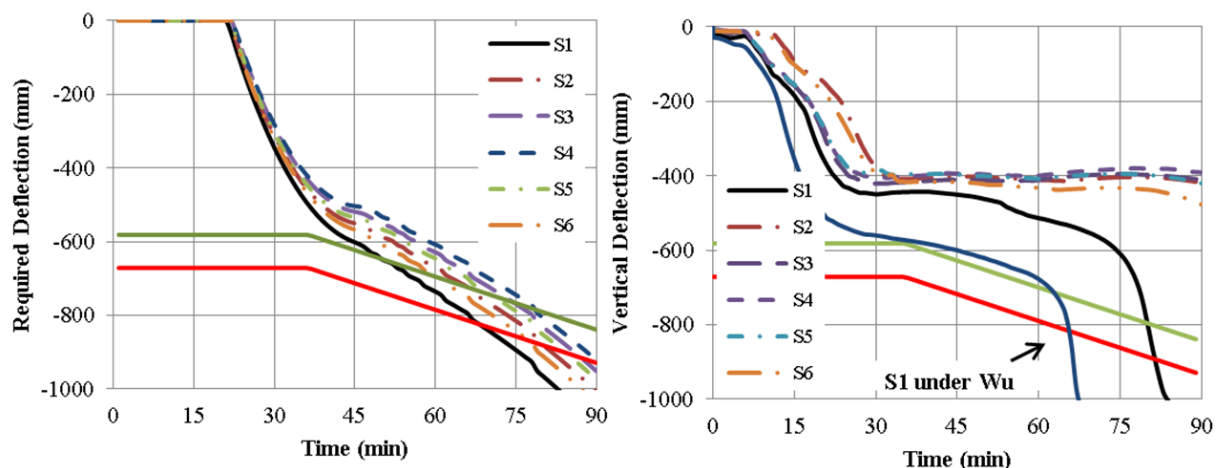


Figure 4-18: SPM – 9 m x 12 m slab panel, required deflections (Left) and VULCAN – 9 m x 9 m slab panel, central vertical deflections (Right).

4.4.3 9 m x 6 m Slab Panel

4.4.3.1 9 m x 6 m Isolated Slab Panel

A 9 m x 6 m isolated slab panel was then modelled. Figure 4-19 compares its SPM limiting and maximum deflections with VULCAN modelled slab panel under its SPM capacity loading. It demonstrated the SPM maximum deflection gave good agreement with the central deflection at 60 minutes. After 60 minutes, the relative secondary beam start decreasing which means the slab panel started collapsing.

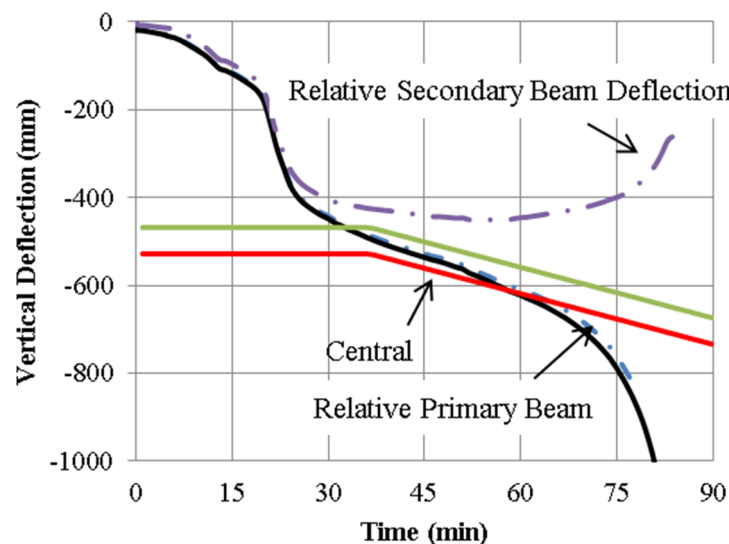


Figure 4-19: 9 m x 6 m comparison between the SPM and the VULCAN central deflection

4.4.3.2 9 m x 6 m Slab Panel with Various Continuities

Figure 4-20 includes all the scenarios of 9 m x 6 m slab panel with different number of continuous edges. The SPM required deflection of these slab panels were calculated and also modelled in VULCAN, as shown in Figure 4-21. The comparison shows the SPM required

deflections were slightly lower than the VULCAN deflection. Therefore, it indicates that the SPM design was not conservative on the 9 m x 6 m slab panel, again because of the edge beam deflections.

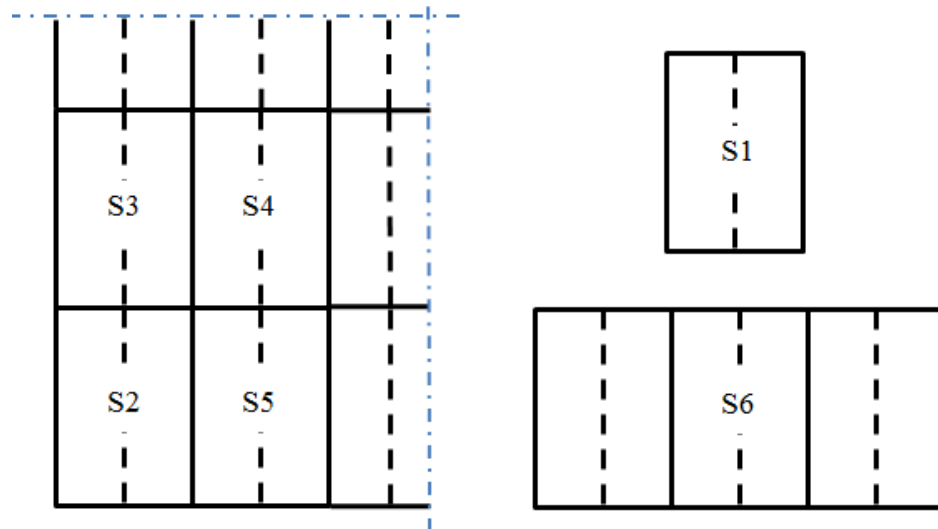


Figure 4-20: 9 m x 6 m slab panels with different number of internal edges from S1 to S6

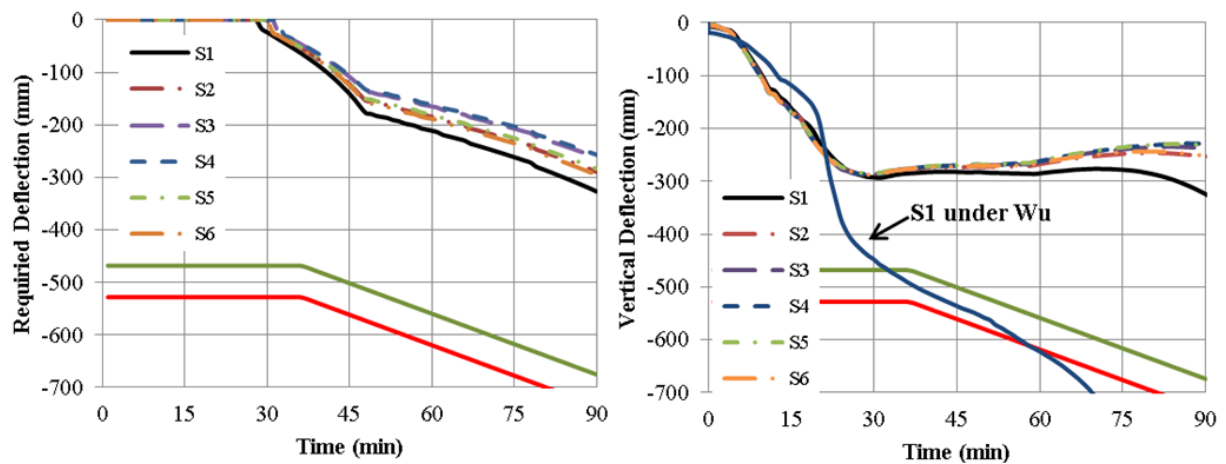


Figure 4-21: SPM – 9 m x 6 m slab panel, required deflection(Left) and VULCAN – 9 m x 6 m slab panel, central vertical deflection (Right).

Conclusions

As illustrated above, a 9 m x 9 m slab panel was modelled in the SPM and VULCAN. VULCAN deflections and the SPM deflections were compared with each other. From the comparisons:

- The VULCAN modelled slab panels demonstrated the whole slab panel became more stable with more continuous edges.
- The results suggested the SPM's prediction was conservative except for an isolated slab panel due to the pre-mature failure of the edge beams, , where it is important that the edge beams are designed to be sufficiently stiff and strong to meet the span/75 limit built into the SPM procedure.
-
- A re-designed slab panel was designed to enhance the edge beam of the 9m x 9m slab panel. The VULCAN deflection of the re-designed slab panel showed good agreement the SPM limiting deflection.
- The SPM required deflection was calculated and compared with the slab panel under fire limit state loading. The SPM required deflections showed same behaviour due to the effect of various continuities.
- Other two slab panels 9 m x 12 m and 9 m x 6 m were modelled to investigate the effect of the aspect ratio. The results demonstrated that the SPM had good agreements to the 9 m x 9 m and 9 m x 12 m slab panels but provided conservative results to the 9 m x 6 m slab panel.

5 CONCLUSIONS AND RECOMMENDATIONS

This research was conducted to study the behaviour of composite floors under fire conditions. The main objectives of this research were to investigate the SPM's provision of edge beam deformations under effect of various edge conditions. The study was performed with Finite Element Analysis (FEA) software VULCAN and the SPM. A series of VULCAN and SPM modelling on slab panels under different support conditions and aspect ratios were undertaken.

The main finds of this research are as follows:

1. The results have shown that edge secondary beams are critical to the fire resistance of the slab but SPM underestimates their deflections if the design is based only on the yieldline tributary area loading. The failure of edge secondary beams would lead to single curvature folding failure mechanism. It was found that the edge beams must be designed for higher loading when using the SPM. This was recognised in the 2014 modifications to the SPM procedure (Clifton and Abu 2014), in which enhanced loading on the edge beams is recommended.
2. After re-designing the edge beams under SPM's capacity load W_u , the comparison between VULCAN and the SPM modelling showed that the SPM's limiting and maximum deflections were in good agreement with VULCAN. However, although the slab panel midspan deflection was well predicted, the SPM underestimated the contribution of the edge beams.

3. The VULCAN models confirmed that continuity of reinforcement over the concrete slab substantially enhanced the stiffness of edge beams. Slab panels with three internal edges (S3 and S5) have less deflections than those with two internal edges (S2 and S6) within the period of fire resistance rating, and also slab panels with three internal edges stay in place longer than those with two internal edges.
4. Comparing slab panels with three internal edges, S5 performed better than S3 because the internal primary beams is stronger than internal secondary edge beam. The internal primary beams are able to undertake the load transferred from the interior secondary beams that lose strength in fire. Comparing slab panels with two internal edges, S6 fails faster than S2 because the internal secondary beams are restrained and the loads are transferred to the external primary beams.
5. The behaviour of slab panels with different aspect ratio were shown the same in VULCAN. However, with different aspect ratio, the accuracy of the SPM varied. The SPM and VULCAN deflections were in good agreement in the 9 m x 9 m slab panel, but SPM underestimated the deflections of 9 m x 6 m slab panel and was slightly conservative on the 9 m x 12 m slab panel. Therefore, SPM is better at designing larger slab panels.
6. SPM is not suitable for isolated slab panels under edge beams designed only for the yieldline tributary area loading. The edge beams in the isolated slab panel needs to be designed for higher loading and recommendations have been made. However in reality the slab panel always has internal edges, the slab continuity over the edge beams provide extra stiffness, therefore the SPM is suitable for all edge support conditions of slab panels in a real floor provided the external edge beams are designed for the increased loading.

7. Although SPM predicts conservative central deflections under any support condition, but it does not predict conservative edge beam deflections. Therefore, to improve the external edge condition, the external edge beams need to be designed under the SPM capacity load to be stronger. It is also recommended to use FEA software along with SPM to check the results.
8. In a structural fire engineering project, using SPM can unprotect many steel beams and still achieve the required fire resistance rating effectively. This is much cheaper than the traditional design. However, the cost of edge beam would be more expensive than conventional structural design because bigger steel beam sizes are needed or more passive fire protection is required. This is a minor additional cost.

5.1 Recommendations for future research

The following areas should be investigated in future research projects:

1. This research only compared the SPM results with VULCAN. Future research can be conducted to investigate the differences between the SPM and the Bailey – BRE method. This can be undertaken by modelling slab panels with the SPM and the Bailey – BRE method with the same structural arrangement within both models, as well as VULCAN.
2. In each size, only one slab panel was modelled by VULCAN and the scenarios with different support conditions were presented by adjusting the rotational restraint of the boundaries. The results are expected to be the same as modelling the full floor. However, to improve the accuracy, full floor is recommended to be modelled in future research.

3. In VULCAN, 1 m × 1 m mesh size was adopted in order to obtain results with acceptable accuracy but also appropriate runtime. However, the accuracy of numerical modelling in VULCAN is largely dependent on the mesh size used in the model. During the validation stage, it was shown that 0.5m x 0.5m mesh size can properly model the Gaston test and gave model stability. Therefore, further research with finer mesh sizes is recommended to be undertaken.
4. In this research, only one reinforcement A193 was used. Abu et al (2012) has done research on the effect of reinforcement ratio on slab panels in fire by assessing the Bailey method accuracy with various reinforcement sizes. Further investigation on slab panel with different reinforcement sizes in the SPM can be conducted to assess the influence of reinforcement ratio on the SPM predictions.

REFERENCES

- ABAQUS 6.10 [Computer software]. (2010). Providence, RI, USA: Dassault Systèmes, Simulia Corporation.
- Abu, A. K. (2009). *Behaviour of Composite Floor Systems in Fire* (Phd thesis). University of Sheffield, Sheffield, UK.
- Abu, A. K., Burgess, I. W., & Plank, R. J. (2008). Slab panel vertical support on tensile membrane action. *Steel and Composite Structures*, 8(3), 217-230.
- Bailey, C. G. (2003). *New fire design method for steel frames with composite floor slabs*. UK Building Research Establishment (BRE).
- Bailey, C. G., & Toh, W. (2007). Behaviour of floor slabs at ambient and elevated temperatures. *Fire safety Journal*, 42(6 - 7), 425-436.
- Bailey, C. G., White, D. S., & Moore, D. B. (2000). The tensile membrane action of unrestrained composite slab simulated under fire conditions. *Engineering Structures*, 22(12), 1583-1595.
- BIA. (2004). *New Zealand Building Code Handbook Approved Documents*. Wellington: Building Industry Authority.
- Buchanan, A. H. (2001). *Structural Design for Fire Safety*. UK: John Wiley & Sons, Ltd.
- Clifton, C. (2006). *Design of Composite Steel Floor Systems for Severe Fires*. . Manukau City, New Zealand: New Zealand Heavy Engineering Research Association (HERA).
- Clifton, G.C. & A.Abu (2014). Development of the Slab Panel Method. SPM Workshop, Auckland and Christchurch, New Zealand, Steel Construction New Zealand.
- EC2. (2004). Eurocode 4: Design of concrete structures. Part 1.1: General rules and rules for buildings. London: European Committee for Standardization.
- EC3. (2005a). Eurocode3: Design of Steel Structures. Part 1.1: General rules and rules for buildings.
- EC3. (2005b). Eurocode 3: Design of Steel Structures. Part 1.2: General rules – Structural fire design. London: European Committee for Standardization.
- EC4. (2005a). Eurocode 4: Design of composite steel and concrete structures. Part 1.1: General rules and rules for buildings. London: European Committee for Standardization.
- EC4. (2005b). Eurocode 4: Design of composite steel and concrete structures. Part 1.2: General rules – Structural fire design. London: European Committee for Standardization.
- Franssen, J.-M. (2005). SAFIR: A thermal/structural program for modelling structures under fire. *Engineering Journal-American Institute of Steel Construction Inc*, 42(3), 143-158.

- Franssen, J.-M., Kodur, V., & Zaharia, R. (2009). *Designing Steel Structures for Fire Safety*. London, UK: CRC Press.
- Huang, Z., Burgess, I. W., & Plank, R. J. (2003a). Modeling Membrane Action of Concrete Slabs in Composite Buildings in Fire. I: Theoretical Development. *Journal of Structural Engineering*, 129(8), 1093 - 1102.
- Huang, Z., Burgess, I. W., & Plank, R. J. (2003b). Modeling Membrane Action of Concrete Slabs in Composite Buildings in Fire. II: Validations. *Journal of Structural Engineering*, 129(8), 1103 - 1112.
- Johansen, K. W. (1962). *Yield-line theory*. London: Cement and Concrete Association.
- Lennon, T. (1996). *Cardington Fire Tests: Instrumentation Locations for Large Compartment Fire Test, Building Research Establishment Report N100/98*. Watford, UK: Building Research Establishment.
- Lim, Z. Y., & Clifton, C. (2012). *Testing of Slab Panel Method program in Severe Fire*. Department of Civil and Environmental Engineering, University of Auckland.
- Moy, S. S. J. (1996). *Plastic methods for steel and concrete structures* (Second ed.). London UK: MacMillan.
- Newman, G. M., & Lawson, R. M. (1991). *Fire Resistance of Composite Beams, Technical Report SCI-P-109*. Steel Construction Institute, Ascot.
- Oehlers, D. J., & Bradford, M. A. (1995). *Composite steel and concrete structural members: fundamental behaviour*. Kidlington, Oxford, UK; Tarrytown, NY: Pergamon.
- Park, R. (1964a). Tensile membrane behaviour of uniformly loaded rectangular reinforced concrete slabs with fully restrained edges. *Megazine of Concete Research*, 16(46), 39-44.
- Park, R. (1964b). The ultimate strength and long-term behaviour of uniformly loaded, two-way concrete slabs with partial lateral restraint at all edges. *Megazine of Concete Research*, 16(48), 139-152.
- Park, R., & Gamble, W. L. (2000). *Reinforced concrete slabs* (2nd ed.). New York: Wiley.
- Powell, D. S. (1956). *Ultimate strength of concrete panels subjected to uniformly distributed loads* (Phd thesis). Cambridge University.
- Purkiss, J. A., & Li, L. (2013). *Fire Safety Engineering Design of Structures* (Third ed.). UK: Taylor & Francis Group, LLC.
- Sawczuk, A., & Winnicki, L. (1965). Plastic behaviour of simply supported reinforced concrete plates at moderately large deflections. *Internaitional journal of Solids and Structures*, 1, 97-111.
- SNZ. (1997). NZS3404: Steel Structures Standard, Parts 1 & 2. Wellington: Standards New Zealand.
- SNZ. (2006). NZS3101: Concrete structures Standard: Standards New Zealand.

Wang, Y. C. (2002). *Steel and Composite Structures: Behaviour and design for fire safety*. USA and Canada: Spon Press.

Wang, Y. C., Burgess, I. W., Wald, F., & Gillie, M. (2013). *Performance-Based Fire Engineering of Structures*. UK: CRC Press.

Wang, Y. C., Lennon, T., & Moore, D. B. (1995). The behaviour of steel frames subject to fire. *Journal of Constructional Steel Research*, 35(13), 291-322.

Wood, R. H. (1961). *Plastic and elastic design of slabs and plates*. London: Thames and Hudson.